

Contents

II	Important Physics Opportunities and Goals	9
1	Introduction and Overview	9
1.1	Introduction	9
1.2	Weak Interactions	10
1.3	QCD	11
1.4	Theoretical Techniques	12
1.4.1	The Lattice	12
1.4.2	Heavy Quark Expansions	13
1.4.3	Models	13
2	Strategy: Why CLEO-c? Why now?	14
3	Charm Decays	15
3.1	Introduction	15
3.2	Leptonic and Semileptonic Decays of Charm	15
3.2.1	Introduction	15
3.2.2	Leptonic Decays	17
3.2.2.1	Motivation and Present Experimental Status	17
3.2.2.2	Leptonic Decays in CLEO-c	19
3.2.3	Semileptonic Decays	20
3.2.3.1	Introduction	20
3.2.3.2	Exclusive Semileptonic Decays	22
3.2.3.3	Inclusive Semileptonic Decays	22
3.2.4	Combined Results and Implications of the Leptonic and Semileptonic Measurements for CKM	23
3.3	Absolute Hadronic Charm Meson Branching Fractions	25
3.3.1	Introduction	25
3.3.2	Current Status	25
3.3.3	Physics Enabled by Better Charm Hadron Branching Fraction Measurements	26
3.3.3.1	Value of $ V_{cb} $	26
3.3.3.2	Understanding Two-body B Meson Decays	27
3.3.3.3	The Charm Content in b Decay	27
3.3.3.4	Effects on Probes of Beyond SM Physics	28
3.3.3.5	QCD Models of Heavy Quark Production	28
3.4	Charm Baryons	28
3.5	Charm Beyond the Standard Model	29
3.5.1	Mixing	29
3.5.2	CP Violation	32
3.5.2.1	Introduction	32
3.5.2.2	Direct CP Violation	32

3.5.2.3	Observing CP Violation Through Quantum Correlations at the ψ''	34
3.5.2.4	Conclusions	34
3.5.3	Rare Charm Decays	34
4	Opportunities for Tau Lepton Physics	35
4.1	Introduction	35
4.2	Measurement of Key Tau Lepton Properties	37
4.2.1	Tau Lepton Mass	37
4.2.2	Tau Decay Branching Fractions	37
4.2.3	Tau Neutrino Mass	39
4.3	Studies of Weak Couplings and Lepton Universality	39
4.3.1	Tests of Lepton Universality	39
4.3.2	Weak Couplings: The Michel Parameters	40
4.4	Studies of Hadronic Dynamics in Tau Decays	41
4.5	Direct Searches for Non-Standard Model Physics	42
4.5.1	Search for $\tau^- \rightarrow \pi^- \nu_X$	42
4.5.2	Search for $\tau^- \rightarrow e^- G$	42
4.5.3	Study of the radiative decay $\tau^- \rightarrow e^- \bar{\nu}_e \nu_\tau \gamma$	43
4.5.4	CP Violation in Tau Decay	43
4.6	Summary of Tau Physics Opportunities	43
5	Nonperturbative QCD	44
5.1	Experimental Probes	44
5.1.1	The $c\bar{c}$ and $b\bar{b}$ States: Well-understood or Not?	45
5.1.2	Exotica: Searches for New Forms of Matter	46
5.1.2.1	Searches for Exotics: Glueballs	48
5.1.2.2	Searches for Exotics: Hybrids	49
5.1.3	Physics Running at the $\psi'(3686)$	50
5.1.3.1	Radiative transitions	50
5.1.3.2	Searches for missing $c\bar{c}$ states	50
5.1.3.3	Exotica from hadronic decays of ψ' and χ_c	52
5.1.3.4	Hadronic branching fractions	52
5.1.4	Summary	53
5.2	Measurement of R	53
	Footnotes and References	54

II Important Physics Opportunities and Goals

1 Introduction and Overview

1.1 Introduction

The modern theory of the weak interactions reached its mature form around 1970 with the unified description of the weak and electromagnetic interaction we refer to as the Standard Model. Since then it has achieved many triumphs, and the verification of the Standard Model has dominated experimental high energy physics for over three decades.

The quark sector of the Standard Model is particularly rich. The phenomenon of quark flavor mixing, first observed among the light quarks in the 1960's [1] and later extended to three generations [2] provides a mechanism to account for the observed CP violation in the K meson system and predicts observable CP violation in the B meson system. A detailed understanding of all aspects of quark flavor mixing is a high priority goal of the world's high energy physics community.

In this proposal we outline a three-year physics program that will contribute to our goal of understanding flavor mixing in two major ways. First, we will describe a suite of measurements involving mesons containing charm quarks that will either directly probe aspects of flavor mixing in the quark sector or enable precision probes at other experiments. We will describe:

- 1 – 2% measurements of $|V_{cs}|$ and $|V_{cd}|$ that provide tests of CKM unitarity, independent of and in some ways orthogonal to the probes of CKM that will be pursued at the B-factories.
- a series of precision measurements of absolute branching ratios, such as $D^0 \rightarrow K^- \pi^+$, $D^+ \rightarrow K^- \pi^+ \pi^+$, $D_s \rightarrow \phi \pi$ and $\Lambda_c^+ \rightarrow p K^- \pi^+$ that will enable precision tests of weak decays that will be done at the B-factories and future hadron facilities.
- probes of physics beyond the Standard Model via searches for rare τ and D decays as well as studies of $D\bar{D}$ mixing and CP violation, that are unique to this program.

A second major goal of this three year program is to provide the experimental data to enable a comprehensive mastery over nonperturbative QCD and to calibrate and validate the theoretical technology that will be necessary for precision flavor physics and will quite likely be crucial for understanding new strongly coupled theories of the future. A major barrier to all studies of heavy flavor physics results from the fact that the physical states of nature are not free quarks, but hadrons: $q\bar{q}$ or qqq bound states where the quarks are confined by the strong interactions. The effects of the strong interactions, nonperturbative QCD, permeate every experimental measurement involving quarks and are an obstacle in almost every attempt to extract precision electroweak physics from data. In addition, as one looks to the future and the next generation of energy-frontier accelerators, it is clear that mastery over strongly-coupled, nonperturbative theories must be established. Most (if not all) popular beyond-the-Standard Model scenarios rely crucially on strong coupling in some sector of the theory. We will describe:

- precision studies of Υ and J/ψ spectroscopy (masses, leptonic widths, branching fractions) that provide a rich testing ground and detailed verification of the theoretical techniques needed to deal with strongly coupled theories.
- measurements of D decay constants and form factors using leptonic and semileptonic decays that will allow stringent calibration of the theoretical techniques needed to provide 1-2% accuracy on theoretical inputs for precision B physics.
- direct probes of the low energy spectrum of QCD using radiative J/ψ decays with precision never before possible, and with particular emphasis on the exotic (glueball and hybrid) part of the spectrum.

The remainder of the introduction will focus on a very brief summary of the major physics thrusts of the program and a brief description of the theoretical techniques needed to elucidate the physics.

1.2 Weak Interactions

A major theme of particle physics in the next decade will be the systematic study of the weak interactions that mix quark and lepton flavors. In the Standard Model, quark flavor mixing is described by the 3×3 unitary Cabibbo-Kobayashi-Maskawa matrix [1],[2]. Its elements are not specified by theory, but rather are the consequence of as yet unknown physics beyond the Standard Model. Experimental programs making measurements of many elements of the CKM matrix, particularly the elements in the third row and third column, are being carried out all over the world.

High energy physics has reached a new milestone in the study of quark flavor mixing with the observation of CP violation in the decay $B \rightarrow J/\psi K_s$ by the asymmetric B-factories at SLAC and KEK [3,4]. Ultimately, if these measurements agree with expectation, we will have passed a major checkpoint. If the measurements disagree with expectation, we will have to begin to redraw the road maps. In either case, once the milestone of a measurement of $\sin 2\beta$ in B decay is passed, heavy quark physics will contribute to our understanding of the Standard Model and what lies beyond almost exclusively through precision measurement. An integral part of the global program in heavy quark physics will be precision measurements in the charm system which are necessary for precision measurements in the B meson system. The charm measurements also serve to calibrate the theoretical techniques used to extract weak physics from the data. Additionally, we can use the charm system to perform tests of our understanding of flavor mixing that are independent of the studies being done in the B meson system.

In this proposal we will describe a physics program that will contribute to this global attack on the physics of heavy flavor mixing. We will describe measurements that probe the essential nature of the weak decays of charm mesons and flavor mixing by clean, high statistics studies of semileptonic charm decays and $D\bar{D}$ mixing. We will describe precision measurements of branching fractions that will set the absolute scale and validate the theoretical techniques for much of the flavor physics done in the next decade, and we will describe direct searches for physics beyond the Standard Model unique to this program.

1.3 QCD

The modern history of strong interaction physics began in the 1960's with the quark model. Initially quarks were regarded merely as mathematical devices that simplified the group theory used to understand hadronic spectra. By the middle of the next decade, however, quarks became an integral part of a new dynamical model for hadronic structure in which hadrons are composed of triplets of quarks, or quark-antiquark pairs, bound together by a new force carried by gluons.

The theory of quarks and gluons is quantum chromodynamics or QCD. QCD is a gauge theory modeled after quantum electrodynamics (QED), with quarks playing the role of electrons, and gluons playing the role of photons. There are two crucial differences between QCD and QED. First, gluons carry QCD charge, while photons are electrically neutral. Consequently Maxwell's equations for QCD are nonlinear in the gauge fields. The second difference is that the QCD charge carried by the quarks in a hadron is an order of magnitude larger than the electrical charge carried by an electron. The combination of strong coupling and nonlinearity makes the low-energy behavior of QCD profoundly different from that of QED. In particular, quarks and gluons are permanently confined inside hadrons.

There were no analytic techniques available for solving strongly-coupled theories like QCD when it was invented. The theory was saved from practical irrelevance by asymptotic freedom: the effective charges of quarks and gluons involved in high-energy collisions decrease with increasing momentum transfer. Consequently deep-inelastic interactions of quarks and gluons can be analyzed with the same perturbative techniques as used in QED. Perturbative QCD has been spectacularly successful in accounting for the observed properties of high-energy quark and gluon jets, and deep-inelastic hadronic cross sections [5]. The quantitative verification of QCD rests largely on such processes.

Although well-established experimentally, the QCD of perturbative quark and gluon jets is the least interesting aspect of the theory since it is quite similar to perturbative QED. The truly novel behavior in QCD is confinement, and confinement is a low-energy, nonperturbative phenomenon.

The theoretical analysis of strongly-coupled, nonperturbative quantum field theories remains one of the foremost challenges in modern physics. It is essential for a complete understanding of QCD, and will quite likely be crucial for understanding the new theories that will be revealed in the next generation of energy-frontier accelerators. It is also a roadblock to investigations in many areas of condensed matter (such as the Kondo effect) and atomic physics (such as very highly ionized systems), where strongly-coupled systems often arise. Much remains to be done. Techniques for rigorous analyses of strongly-coupled field theories, such as lattice QCD or strong-coupling techniques inspired by string theory, are still in the early stages of their development. Additionally, *ab initio* calculations, using, for example, lattice QCD, are expensive and time consuming, and the results are incomplete. Consequently, a variety of other theoretical strategies are required to both complement and supplement lattice analyses. These range from rigorous expansions such as heavy quark or chiral expansions to phenomenological models that combine existing data with various theoretical aspects of QCD to provide insights about complex nonperturbative phenomena, together with simple frameworks for both qualitative and semi-quantitative analyses. Often the models can serve to guide the lattice and other more rigorous techniques and have the

advantage of illuminating the physics in a more accessible fashion and helping to develop our intuition about the problems we are trying to address.

For most of its history, practical quantum field theory has been synonymous with perturbative quantum field theory. A comprehensive demonstration of our mastery over non-perturbative QCD, particularly if it is at the level of 1% errors, would be a landmark in the history of quantum field theory. The experimental program outlined in this proposal would provide the experimental basis for this demonstration.

1.4 Theoretical Techniques

1.4.1 The Lattice

The lattice version of QCD is the only complete definition of the theory, encompassing both perturbative and nonperturbative aspects of the theory. Lattice QCD was invented in the earliest days of QCD, when it provided the first qualitative understanding of quark confinement. The theory was largely unproductive for the next fifteen years. This situation changed dramatically in the early 1990's, when serious technical problems were identified and overcome [6], and, especially in the last five years, as substantially improved algorithms were developed and widely adopted [7]. Consequently lattice QCD, despite its age, is just now growing out of its infancy. A wide variety of nonperturbative quantities has now been analyzed with precisions of order $\sim 15\%$. These include glueball and hybrid-meson masses, form factors, and decay constants for a wide range of conventional hadrons. The techniques for lattice QCD continue to evolve rapidly; next-generation results for many of these quantities will be accurate to $\sim 1\%$.

The “gold-plated” quantities, for which lattice QCD can achieve $\sim 1\%$ precision within the next few years include the static properties and electroweak form factors of any hadron that is stable or nearly stable with respect to QCD interactions [8]. The list includes:

- the masses, leptonic widths, electromagnetic transition form factors, and mixing amplitudes for any meson in the Υ and J/ψ families below B and D threshold, respectively;
- the masses, decay constants, semileptonic form factors, and mixing amplitudes for the D , D^* , B and B^* mesons, and for the analogous mesons with strange quarks;
- the masses and semileptonic form factors of low-lying baryons containing c and b quarks;
- masses, decay constants, electroweak form factors, charge radii, magnetic moments, and mixing amplitudes for the low-lying light-quark mesons and hadrons, with and without strange quarks.

Comparisons of numerical results on Υ and J/ψ spectra with similarly accurate experimental results would provide invaluable tests of lattice QCD methods. They would allow experimental calibration of the accuracy of the B and D results that are crucial to the experimental program in heavy-quark physics; and they would drive further refinements of the lattice methods.

Lattice techniques are less well developed for hadrons with QCD decay widths of order 50 MeV or more. So far, many of the properties of these hadrons have been computed only in the quenched approximation to the theory, where quark vacuum polarization is omitted, and this typically limits precision to 10-20%. Rigorous techniques exist for analyzing unstable hadrons and for computing partial widths to different decay channels with fully unquenched

calculations. These are costly and so far still in the prototype stage. Recent improvements in lattice algorithms probably make it feasible to apply these methods to glueballs and hybrid mesons using next-generation lattice computing facilities. The limitations of current experimental data have provided little incentive in the past to develop these powerful but costly techniques. This situation will change dramatically with the arrival of the data described in this proposal.

1.4.2 Heavy Quark Expansions

When studying processes involving physical hadrons, there are often several contributions to the process from different energy scales. For example, the weak decay of a b quark takes place at the scale defined by the mass of W boson, or at relative distances of about $1/M_W$, while the soft interaction between a b quark and a spectator inside the hadron happens at the much larger distances of $1/\Lambda_{QCD}$. Therefore, from the point of view of the larger scale, anything that occurs at much shorter scales can be well approximated by a point-like interaction. This concept can be called *scale separation* and allows for expansions of various quantities in the ratios of those scales. The rigorous non-perturbative technique behind this simple idea goes by the name of Operator Product Expansion (OPE). It was successfully applied in the past to study the processes such as deep inelastic scattering. For example, this method allows us to compute $1/Q^{2n}$ power corrections to asymptotic values of physical observables computed in perturbative QCD.

Similar analyses can be extended to study decays of heavy quarkonia and heavy mesons with open flavor, like B or D mesons, where the large value of transferred momentum is provided by the decaying heavy quark [9]. Therefore, many physical observables, like the inclusive decay rate, can be computed in terms of an expansion in inverse powers of heavy quark mass.

It is often convenient to redefine the field content of the theory by scaling out the large mechanical component of the heavy quark field and deriving an *effective field theory*, like HQET or NRQCD. These theories enjoy invariance under larger spin-flavor symmetry groups than QCD and can be derived from it in the appropriate heavy quark limit. A set of symmetry-violating corrections can then be computed as expansion governed by the relevant parameter like $1/m_Q$ (HQET) or relative heavy quark velocity v (NRQCD).

Of course, effective theories do not solve QCD, but rather separate computable, semi-perturbative parts of the observables from truly non-perturbative, but *universal* parameters. A multitude of these parameters can be measured at CLEO-c. For example, many parameters (matrix elements) of the NRQCD expansion are universal, *i.e.*, govern both decay and production of heavy quarkonium states [10]. The accurate extraction of these parameters (*e.g.*, in quarkonium leptonic and inclusive decays) is important for understanding the limits of applicability of these theories as well as for the extraction of more fundamental parameters of the Standard Model Lagrangian, like CKM matrix elements.

1.4.3 Models

Models use different approaches to highlight different aspects of QCD, and frequently involve extrapolations from unphysical limits of QCD that are analytically tractable. For

hadronic physics constituent-quark models which become precise in the limit of large quark mass, are used to compute the mass spectra of both normal and exotic hadrons. That it works well for heavy mesons is not surprising. By a happy accident of nature which we would like to understand in more depth, it has also proved remarkably accurate for light mesons. Flux-tube models, in which quarks are connected by dynamical QCD-flux tubes, are inspired by the strong-coupling (large-lattice-spacing) limit of lattice QCD (and also by superconductivity) [11] and provide a close link between the lattice and hadron spectroscopy.

Most current models have been carefully tuned so that they are consistent with the known properties of standard mesons and baryons. Consequently the most powerful way to discriminate between them is to test their predictions against accurate results for nonstandard mesons, and in particular for glueballs and hybrid mesons. Accurate experiments will guide us to the correct qualitative pictures, and these qualitative pictures will provide the basis upon which we will develop rigorous techniques in the future.

2 Strategy: Why CLEO-c? Why now?

The concept of an experimental program dedicated to high statistics studies of tau and charm (a so-called “tau-charm factory”) was discussed vigorously in the 1990’s. The end of the MARK-III program in the late 1980’s left a great deal of physics undone. The BES program has helped to fill in some of the gaps but the modest luminosity of the BEPC machine ($\sim 5 \times 10^{30} \text{ cm}^{-2} \text{ s}^{-1}$) and limited running time have resulted in a program with a physics reach that is not dramatically deeper than the original MARK-III program. Workshops at SLAC in 1989 [12], Seville in 1991 [13], Marbella in 1993 [14], Argonne in 1995 [15], and again at SLAC in 1999 [16], focussed on modern detectors operating at electron positron colliders with luminosities in excess of $\sim 10^{33} \text{ cm}^{-2} \text{ s}^{-1}$ at $\sqrt{s} \sim 4 \text{ GeV}$, and explored strategies to use tau and charm studies to either “strengthen the experimental foundations underpinning the Standard Model or potentially provide a breakthrough to the New Physics beyond” [14].

The rise of the asymmetric B -factory proposals and the construction of the machines in the mid- to late-1990’s effectively put an end to discussions of a tau-charm factory in the US or Europe. The B mesons provided a more direct route to testing our understanding of heavy flavor mixing and provided rich opportunities in charm and tau physics as well. Fundamentally, for probing the underlying structure of the weak interactions of heavy quarks, the B system looked to be a better bet.

The experimental program we are proposing here is not a tau-charm factory in the terms that have been discussed for the past decade. While the detector is comparable to the tau-charm factory detectors, the machine luminosity is less; the CLEO-c program relies on CESR operating at $1 - 5 \times 10^{32} \text{ cm}^{-2} \text{ s}^{-1}$ which is more than an order of magnitude above what BEPC is achieving but almost a factor of three below the tau-charm factory goals. The cost of the CLEO-c program is dramatically less. Estimates for the CESR-c conversion are under 5M\$ while the estimates for a tau-charm factory were of order 100M\$ for the machine component. The physics goals of CESR-c are also quite different from the original tau-charm goals. Rather than directly challenging the Standard Model paradigm for quark mixing, the CLEO-c program is focussed on enabling the precision flavor physics at other machines and on providing experimental data to confront the ability of our theoretical technology

to address nonperturbative QCD. This program is fully achieved with the more modest luminosity goals of CESR-c in approximately three years of data taking. Furthermore, Υ and two-photon data taken at 10.6 GeV before the CLEO-c conversion which were not part of the 1990's tau-charm proposals, are essential elements of the program.

It is appropriate to ask whether the physics goals of the CLEO-c program could be achieved at other existing or planned facilities. Certain individual measurements in the planned CLEO-c physics program are accessible from other machines and comparisons will be detailed in Chapter III. In general, however, the high statistics, low background environment available when running at charm threshold allows significantly higher precision for the decays being targeted by this program. In addition, if one views the ultimate goal of CLEO-c as providing the data necessary to establish comprehensive mastery over nonperturbative QCD, the program is unique. The Υ and J/ψ parts of the program provide the most efficient testing ground for lattice techniques. The precision leptonic and semileptonic charm meson measurements are essential to provide credibility and viability in the application of the theoretical techniques to the bottom system for measurements of, for example, $|V_{ub}|$. The convergence of the experimental opportunity of CLEO-c with the "lattice revolution" of the last decade is generating intense enthusiasm for the program from the lattice community. The CLEO-c program will force the theoretical community to confront precision data in open- and hidden-flavor charm and hidden-flavor bottom mesons simultaneously, and it will be happening at a time when theorists are ready to meet the challenge.

3 Charm Decays

3.1 Introduction

The observable properties of the charm mesons are determined by the strong and weak interactions. As a result, charm mesons can be used as a laboratory for the studies of these two fundamental forces. The challenge, often, is to separate the weak physics which controls the decays of these mesons from the effects of nonperturbative QCD which binds the quarks to make the physical mesons in the initial and final states. Threshold charm experiments permit a series of measurements that enable direct study of the weak interactions of the charm quark as well as tests of our theoretical technology for handling the strong interactions. In this section we will review the physics that drives the experimental studies. In Chapter III we will detail the capabilities of CLEO-c to perform them.

3.2 Leptonic and Semileptonic Decays of Charm

3.2.1 Introduction

The mixing of flavors and generations induced by weak interactions is of profound importance to our understanding of the universe we live in. This mixing is summarized for three generations by the standard Cabibbo-Kobayashi-Maskawa (CKM) matrix, whose elements are fundamental parameters not predicted within the Standard Model and must be determined by experiment. Although 3-generation unitarity is often assumed in discussions of the CKM matrix, actual *direct* measurements of the matrix elements *without* the assumption

of 3-generation unitarity remain highly imprecise for most of the matrix. Below we show the relative uncertainty on the magnitude of each of the matrix elements as they are known today from direct measurement [17].

<u>CKM Matrix</u>			<u>Relative Uncertainty</u>		
V_{ud}	V_{us}	V_{ub}	0.1%	1%	25%
V_{cd}	V_{cs}	V_{cb}	7%	16%	5%
V_{td}	V_{ts}	V_{tb}	36%	39%	29%

(1)

Determination of the magnitudes and phases of the elements of this matrix continues to be the principal goal of experimental effort across the whole spectrum of heavy quark experiments, from rare kaon decay experiments to B factories to $p\bar{p}$ collider experiments, and precise measurements of the elements of the matrix will underwrite future progress in understanding the mechanisms of CP violation and help point the direction to New Physics in which the Standard Model may be embedded. CLEO-c will make significant contributions to this effort in two distinct ways.

First, CLEO-c will provide a large set of precision measurements in the charm sector against which the theoretical tools needed to extract CKM information precisely from heavy quark decay measurements may be tested and honed. We list below some of these measurements and the larger CKM goals they will enable:

- Measurements of the as yet barely known leptonic decay rates for D and D_s to a precision of 3–4%. These will allow incisive checks of theoretical calculations of the decay constants f_D and f_{D_s} at the 1–2% level. Theories that reproduce the results then can be used to determine f_B and f_{B_s} and their ratio. With this information we can then interpret the B factory and collider measurements of B and B_s mixing parameters and determine the CKM elements $|V_{td}|$ and $|V_{ts}|$ with a precision of about 5%.
- Measurements of the pseudoscalar form factor $f_+(q^2)$ slope and normalization in the decays $D^+ \rightarrow \bar{K}^0 e^+ \nu$, $D^0 \rightarrow K^- e^+ \nu$, $D^+ \rightarrow \pi^0 e^+ \nu$, $D^0 \rightarrow \pi^- e^+ \nu$, and $D_s \rightarrow \eta e \nu$ at the level of 4%. Measurements of the normalization and q^2 dependence of the vector and axial vector form factors $V(q^2)$, $A_1(q^2)$, and $A_2(q^2)$ will also be available at the $\sim 5\%$ level for decay modes such as $D^0 \rightarrow K^{*-} e^+ \nu$, $D^0 \rightarrow \rho^- e^+ \nu$, $D^+ \rightarrow \bar{K}^{0*} e^+ \nu$, $D^+ \rightarrow \rho^0 e^+ \nu$, $D^+ \rightarrow \omega e^+ \nu$, $D_s^+ \rightarrow \phi e^+ \nu$, and $D_s^+ \rightarrow \bar{K}^{0*} e^+ \nu$. Confronted with this broad range of precise experimental information, theoretical calculations of form factors in weak decay can be refined and validated so that in the subsequent application to $B \rightarrow \pi \ell \nu$, one will be able to extract $|V_{ub}|$ to an overall precision of about 5%.
- Measurements of hadronic charm meson branching fractions to 1–2% precision. These measurements will be discussed in a separate Section, but we note here their relevance to the CKM program. Charm meson branching ratios appear as scale factors in determinations of V_{cb} , and present uncertainties in their values will soon be a limiting systematic error in measurements of V_{cb} . In addition to governing our knowledge of the CKM parameter V_{cb} itself, these uncertainties limit our knowledge of the overall strength of coupling between the third generation and the first and second generations (the Wolfenstein A parameter), which in turn affects the width of the swath in (ρ, η) parameter space mapped out by measurements of ϵ_K in kaon CP violation. When we establish the scale of global normalizing modes to 1–2%, we open the door to precision determination of fundamental parameters throughout heavy flavor physics.

It is essential to recognize that the accurate calibration of theoretical techniques for calculating hadronic factors as described above requires control of the *a priori* poorly known CKM factors. This may be done either by assumption (imposing CKM unitarity fixes $|V_{cd}|$ and $|V_{cs}|$ to better than 1%) or by direct elimination. As an example, we note that ratios of rates can offer a straightforward way to scale out CKM factors and provide pure hadronic terms for the theoretical testbeds, without any assumptions required. Thus for instance, the ratio

$$\frac{\frac{d\Gamma}{dq^2}(D^+ \rightarrow \bar{K}^0 e^+ \nu_e)}{\Gamma(D^+ \rightarrow \mu^+ \nu_\mu)} = \left(3\pi^2 m_D m_\mu^2 \left(1 - \frac{m_\mu^2}{m_D^2}\right) \right)^{-1} p_{\bar{K}^0}^3 \frac{|f_+(q^2)|^2}{f_{D^+}^2} \quad (2)$$

cleanly displays the hadronic elements involved in these two weak decays with no additional uncertainty beyond the experimental error bars. This ratio, and similar ratios of other leptonic and semileptonic rates will be valuable in confronting theoretical tools.

In addition to these internal checks which are available with the leptonic and semileptonic decay data, other CLEO-c data taken at the Υ resonances and at the J/ψ resonance can be used to demonstrate the validity and precision of Lattice QCD or other theoretical calculations. This is a particularly useful and relevant cross check because calculations of photon transition matrix elements are closely related to calculations of semileptonic decay form factors, and leptonic widths of onia states are similarly closely related to meson decay constants. These onia measurements are discussed further in Section 5.1.1.

Second, provided the theoretical tools have been satisfactorily checked and validated against the set of calibration data provided by CLEO-c as described above, we may now proceed to extract CKM elements from the CLEO-c data itself. In particular, if the theory achieves a precision of $\sim 3\%$ in the semileptonic form factors, and $\sim 1\%$ in the decay constants, then the following opportunities now open up:

- Measurements of the leptonic decay $D^+ \rightarrow \mu^+ \nu$, together with its semileptonic cousin $D \rightarrow \pi e \nu$. From these data we will extract the CKM element $|V_{cd}|$ with a precision of 1.4%.
- Measurements of the leptonic decays $D_s^+ \rightarrow \mu^+ \nu$ and $D_s^+ \rightarrow \tau^+ \nu$ and semileptonic decays $D \rightarrow K \ell \nu$. These will yield $|V_{cs}|$ with a precision of 1.1% precision.

These measurements will bring our direct knowledge of $|V_{cd}|$ and $|V_{cs}|$ to the same level of precision as we currently know the Cabibbo angle, $|V_{us}|$. Absent assumptions about 3-generation unitarity, our present knowledge of $|V_{cd}|$ and $|V_{cs}|$ is about one order of magnitude worse and will not improve except through the precision determinations of weak charm decays as proposed here.

The CLEO-c program of precision charm physics thus directly or indirectly touches on every CKM measurement except V_{ud} , V_{us} and V_{tb} , and, in concert with the other experiments in the global effort in heavy quark physics, will have a profound effect on our knowledge of this matrix.

3.2.2 Leptonic Decays

3.2.2.1 Motivation and Present Experimental Status

The purely leptonic decays of mesons are as theoretically elegant as they are experimentally challenging. The expression for the branching fraction, ignoring radiative corrections,

is

$$\mathcal{B}(D_q \rightarrow \ell\nu) = \frac{G_F^2}{8\pi} m_{D_q} m_\ell^2 \left(1 - \frac{m_\ell^2}{m_{D_q}^2}\right)^2 f_{D_q}^2 |V_{cq}|^2 \tau_{D_q}. \quad (3)$$

This illustrates the confrontation of weak interaction physics and strong interaction physics that characterizes most issues in the heavy quark field. In the present case the hadronic physics is encapsulated in a single parameter, the decay constant f_{D_q} , that quantifies the amplitude for the valence quarks to be at zero separation, while the weak physics is embedded in the CKM parameter $|V_{cq}|$ that quantifies the amplitude for quark mixing. Both quantities are of great interest. We will discuss the CKM elements further in Section 3.2.4 and pause here to discuss briefly the usefulness of decay constant determinations.

Decay constants appear not only in weak annihilation decay processes such as $M \rightarrow \ell\nu$ but also in mixing amplitudes $\overline{M}^0 \Leftrightarrow M^0$ where the valence quarks must approach within a distance $\sim 1/m_W \ll 1/m_M$ for mixing to occur. Our ignorance of decay constants f_B and f_{B_s} limits for the foreseeable future our ability to extract the interesting CKM elements $|V_{td}|$ and $|V_{ts}|$ from B and B_s mixing frequencies Δm_d and Δm_s :

$$\Delta m_q = \frac{G_F^2}{6\pi^2} \eta_B m_B m_W^2 B_B S_0(\overline{m}_t^2/m_W^2) f_B^2 |V_{tb}|^2 |V_{tq}|^2. \quad (4)$$

Precise measurements of the B_d mixing frequency Δm_d are already available, and corresponding measurements for the B_s mixing frequency Δm_s should be available in a few years. Yet measurements of the decay constants f_B and f_{B_s} remain far in the future and they are unlikely ever to be known to much better than 10%. Precise measurements of the decay constants f_D and f_{D_s} are therefore of interest as we anticipate eventual use of Lattice QCD to compute ratios such as f_B/f_D reliably and thereby scale precise experimental values of f_D and f_{D_s} to obtain precise values of f_B and f_{B_s} . As discussed above, the suite of CLEO-c leptonic, semileptonic, and quarkonia measurements will play an active and essential role in establishing the reliability of the theory for these applications.

In the intermediate term, computations of the ratio f_{B_s}/f_B are already thought to be reliable at the level of $\sim 4\%$ [18], and it is therefore common these days to extract limits on $|V_{td}|$ from the experimental limits on $\Delta m_s/\Delta m_d$. This procedure embodies a hidden assumption of unitarity ($|V_{ts}| \approx |V_{cb}|$) that eventually we will be able to dispense with when we can obtain the decay constants separately.

Measurements of leptonic branching fractions however have long been hampered by small rates and the weak signature of the final state. Even the best measured mode, the Cabibbo-allowed decay $D_s \rightarrow \mu\nu$, is a 35% measurement limited by difficult background systematics and large uncertainties in the branching fraction of the normalizing mode $D_s \rightarrow \phi\pi$. We summarize the present knowledge of leptonic branching fractions in Table 1.

Radiative corrections are expected to contribute an uncertainty which is small compared to the experimental precision quoted above [22] and can be ignored here. We note more generally that radiative leptonic decays such as $D^+ \rightarrow \gamma\ell^+\nu$ have less helicity suppression than their purely leptonic counterparts, and have been suggested as alternative ways to approach the leptonic decays. Unfortunately, in the absence of clean theoretical treatment of the meson structure-dependent terms, extraction of fundamental CKM parameters is compromised. We therefore have chosen to focus on the purely leptonic modes.

TABLE 1. Measured Leptonic Branching Fractions \mathcal{B} .

Decay Mode	\mathcal{B}	$\Delta\mathcal{B}/\mathcal{B}$	Nr. Signal Evts	Exp't.
$D^+ \rightarrow \mu^+\nu$	$(0.08^{+0.16+0.05}_{-0.05-0.02})\%$	$\sim 100\%$	1	BES [19]
$D_s^+ \rightarrow \mu^+\nu$	$(0.62 \pm 0.08 \pm 0.13 \pm 0.16)\%$	35%	182	CLEO [20]
$D_s^+ \rightarrow \tau^+\nu$	$(7.4 \pm 2.8 \pm 2.4)\%$	50%	16	L3 [21]

3.2.2.2 Leptonic Decays in CLEO-c

Measurements of leptonic decays in CLEO-c will benefit from the use of fully tagged D^+ and D_s decays available at the $\psi(3770)$ and at $\sqrt{s} \sim 4140$ MeV. The leptonic decays $D_q \rightarrow \mu\nu$ are detected in tagged events by observing a single charged track of the correct sign, missing energy, and a complete accounting of residual energy in the calorimeter. It is not even necessary to identify the lepton flavor. The crisp definition of the initial state, the cleanliness of the tag reconstruction, and the absence of additional fragmentation tracks make this measurement straightforward and essentially background-free. The decay $D_s \rightarrow \tau\nu$ is more complicated due to the secondary decay of the τ , but substantially more plentiful since the large τ mass lifts the helicity suppression. Details of these measurements will be given in Chapter III where the expected sensitivity of CLEO-c for the leptonic branching fractions is summarized. The actual precision in any mode depends of course on the true branching fraction which, as noted above, is not well known at this point. For our projections we assume $f_D = 220$ MeV and $f_{D_s} = 260$ MeV.

The implications for CKM parameter extraction will be discussed in Section 3.2.4 after we have reviewed the semileptonic decays. We note meanwhile that decay constants may be extracted if we fix the elements $|V_{cd}|$ and $|V_{cs}|$ by assuming 3-generation unitarity. At the present time this gives $|V_{cd}|$ to 1.1% and $|V_{cs}|$ to 0.1%. D^+ and D_s lifetimes are known now to 1.2% and 2.0%. With these values, and with systematic errors as discussed in Chapter III, we summarize the sensitivity for f_D and f_{D_s} in Table 2.

TABLE 2. CLEO-c: Expected Precision in Decay Constants

Decay Mode	Decay Constant	$\Delta f_{D_q}/f_{D_q}$
$D^+ \rightarrow \mu^+\nu$	f_D	2.3%
$D_s^+ \rightarrow \mu^+\nu$	f_{D_s}	1.9%
$D_s^+ \rightarrow \tau^+\nu$	f_{D_s}	1.6%

3.2.3 Semileptonic Decays

3.2.3.1 Introduction

Although measurements of leptonic decays have suffered from experimental obstacles, *semileptonic* decays have long served as an excellent laboratory in which to study both weak physics and QCD physics. The perennial challenge here is to separate the weak physics from the QCD physics.

The expression for the differential decay rate $D \rightarrow K\ell\nu$ is analogous to the leptonic decay rate $D \rightarrow \ell\nu$ given above in Equation (3) and illustrates again the confluence of weak and strong physics in one process:

$$\frac{d\Gamma}{dq^2} = \frac{G_F^2}{24\pi^3} |V_{cs}|^2 p_K^3 |f_+(q^2)|^2. \quad (5)$$

In this case the hadronic physics is captured in the form factor $f_+(q^2)$ which measures the probability that the strange quark and the spectator will form the final state kaon. The weak physics appears in the CKM element $|V_{cs}|$.

Semileptonic decays to vector final states such as $D \rightarrow K^*\ell\nu$ ($K^* \rightarrow K\pi$) exhibit the same meeting of strong and weak physics, but are vastly richer in hadronic complexity:

$$\begin{aligned} \frac{d\Gamma}{dq^2 d\cos\theta_K d\cos\theta_\ell d\chi} &= \frac{3G_F^2}{8(4\pi)^4} |V_{cs}|^2 \times \frac{p_{K^*} q^2}{M_D^2} [(1 + \cos\theta_\ell)^2 \sin^2\theta_K |H_+(q^2)|^2 \\ &+ (1 - \cos\theta_\ell)^2 \sin^2\theta_K |H_-(q^2)|^2 \\ &+ 4 \sin^2\theta_\ell \cos^2\theta_K |H_0(q^2)|^2 \\ &+ 4 \sin\theta_\ell (1 + \cos\theta_\ell) \sin\theta_K \cos\theta_K \cos\chi H_+(q^2) H_0(q^2) \\ &- 4 \sin\theta_\ell (1 - \cos\theta_\ell) \sin\theta_K \cos\theta_K \cos\chi H_-(q^2) H_0(q^2) \\ &- 2 \sin^2\theta_\ell \sin^2\theta_K \cos 2\chi H_+(q^2) H_-(q^2)] \times \mathcal{B}(K^* \rightarrow K\pi). \end{aligned} \quad (6)$$

Here there are angles θ_K , θ_ℓ , and χ to characterize the decay angles of the lepton and kaon, and the relative orientation of the decay planes; as well as three helicity amplitudes, $H_+(q^2)$, $H_-(q^2)$, and $H_0(q^2)$ which are themselves functions of the vector and axial vector form factors. These characterize the probabilities that the strange quark and the spectator will form a K^* with the various indicated helicities.

Compared to leptonic decays semileptonic decays enjoy two distinct advantages. First, they have substantially larger branching ratios and cleaner signatures; and second, they offer more observables, namely overall rate and form factor shape(s) – compared to leptonic decays which manifest rate only. Because of the latter feature, one can use semileptonic decays to study in some depth the two main theoretical treatments of heavy quark decay. Inclusive semileptonic decays test the heavy quark expansion, HQET, while exclusive semileptonic decays test Lattice QCD.

On the other hand, as one moves from the purely leptonic decays described by Equation (3), to the semileptonic (pseudoscalar) decays of Equation (5), and finally to the semileptonic (vector) decays of Equation (6), the demands on both theory and experiment grow substantially. For full application of the theoretical machinery to all semileptonic and leptonic decays however, we will require verification at all points where we can possibly confront theory with data. Hence a broad program of measurements is planned.

Examples of successful CKM extractions in semileptonic decay measurements include $|V_{ud}|$ from nuclear β decay, $|V_{us}|$ from kaon semileptonic decay and $|V_{cb}|$ from $B \rightarrow D^* \ell \nu$. In each case a flavor symmetry – isospin, SU(3), and heavy quark symmetry, respectively – greatly simplifies the theoretical understanding of the hadronic transition matrix element. In the symmetry limit, and at zero recoil, current conservation ensures that the matrix elements are exactly normalized. Deviations from the symmetry limit exist, and may be difficult to calculate, but the deviations tend to be small. Therefore the overall theoretical uncertainty on the decay process is under control. Combined with good experimental measurements, the associated CKM matrix element can be reliably extracted.

But for the critical case of extracting $|V_{ub}|$ from $B \rightarrow X_{u,d} \ell \nu$ the situation is not nearly as clean. In semileptonic decays of the heavy mesons D and B mesons into light mesons like π or ρ , there are no symmetries to constrain the hadronic transition matrix element. Consequently the errors on $|V_{ub}|$ are currently dominated by theoretical uncertainties and are not well known. Recently improved LQCD calculations of the form factors in $D \rightarrow \pi/K \ell \nu$ and $B \rightarrow \pi \ell \nu$ have become available. These calculations represent an important step towards reducing the theoretical error, and may be the best way to obtain precise values of $|V_{cd}|$, $|V_{cs}|$ and $|V_{ub}|$ in the future. But reliance on these theoretical inputs will demand substantial experimental verification if we wish to ensure believably small errors in the final result.

To this end we propose to use charm semileptonic decays as a clean laboratory to isolate and study the effects of non-perturbative QCD on weak decay processes. For this purpose we can either construct ratios of experimental quantities which explicitly eliminate CKM dependence, as in Equation (2), or simply use for this case the assumption of 3-generation unitarity, under which assumption V_{cs} and V_{cd} are already constrained to 0.1% and 1%, respectively. Importantly, measurements can be made for a variety of semileptonic decay modes in the same experiment, allowing cross checks of semileptonic rates from theory with reduced experimental and theoretical systematic errors.

Inclusive semileptonic decays will also be measured in CLEO-c and offer many useful features. The nonperturbative dynamics shaping inclusive semileptonic transitions of heavy flavor hadrons can be treated by heavy quark expansions (HQET) [23] in inverse powers of the heavy quark mass m_Q . Similarly to the studies discussed above there is a dual motivation for analyzing inclusive semileptonic charm decays:

- From the measured inclusive semileptonic width, moments of the lepton spectrum, moments of the hadronic mass spectrum, and the q^2 distribution one can extract $|V_{cs}|$ and $|V_{cd}|$ and compare them to
 - the values obtained from exclusive decays in combination with LQCD and
 - the values inferred from three-family unitarity of the CKM matrix.
 Such a comparison allows us a calibration test of methods used for determining $|V_{cb}|$ and $|V_{ub}|$.
- While HQET should yield a good quantitative description for beauty hadrons, a priori this may not be true for charm decays since the charm quark mass exceeds ordinary hadronic scales by a moderate amount only. It is conceivable that quark-hadron duality, or duality for short, holds effectively only for scales higher than charm and at m_c can yield no better than a qualitative description. Probing the onset of duality provides important lessons in nonperturbative dynamics at scales characterized by m_c in general and on a proper theoretical treatment of $D^0 \bar{D}^0$ oscillations as well as of $B \rightarrow \ell \nu D^*/D$.

In the following Sections we discuss the physics opportunities at CLEO-c with semileptonic decays in greater detail and show how these opportunities are intimately related to other parts of the CLEO-c program. In Chapter III simulations of these measurements are presented.

3.2.3.2 Exclusive Semileptonic Decays

CLEO-c will measure the branching ratios of many exclusive semileptonic modes, including $D^0 \rightarrow K^- e^+ \nu$, $D^0 \rightarrow \pi^- e^+ \nu$, $D^0 \rightarrow K^{*-} e^+ \nu$, $D^0 \rightarrow \rho^- e^+ \nu$, $D^+ \rightarrow \bar{K}^0 e^+ \nu$, $D^+ \rightarrow \pi^0 e^+ \nu$, $D^+ \rightarrow \bar{K}^{0*} e^+ \nu$, $D^+ \rightarrow \rho^0 e^+ \nu$, $D^+ \rightarrow \omega e^+ \nu$, $D_s^+ \rightarrow \eta e^+ \nu$, $D_s^+ \rightarrow \phi e^+ \nu$, $D_s^+ \rightarrow \bar{K}^0 e^+ \nu$, $D_s^+ \rightarrow \bar{K}^{0*} e^+ \nu$. The measurement in each case is based on the use of tagged events where the cleanliness of the environment provides nearly background-free signal samples. Details of the analysis will be discussed in Chapter III, and we summarize the main results here. We use the currently available D and D_s lifetimes, and assume that theoretical control over the hadronic contributions will be accurate to 3%. For the purposes of extracting CKM elements, we will for now limit ourselves to only the simplest pseudoscalar modes where signal yields are highest, backgrounds are lowest, and theoretical contributions will be best understood. More complicated semileptonic modes, such as those involving vector states, will play a role in constraining, testing, and validating theoretical calculations. We summarize in Table 3 the results of the pseudoscalar semileptonic measurements and their associated determinations of CKM parameters.

TABLE 3. CLEO-c: Expected Precision in Semileptonic Decays.

Decay Mode	$\Delta\Gamma/\Gamma$	CKM Element	CKM precision
$D^0 \rightarrow K^- e^+ \nu$	1.2%	$ V_{cs} $	1.6%
$D^0 \rightarrow \pi^- e^+ \nu$	1.5%	$ V_{cd} $	1.7%

Finally we note that some systematic errors may cancel in taking ratios and permit yet more precise information to be extracted. The ratio $\mathcal{B}(D \rightarrow \pi \ell \nu)/\mathcal{B}(D \rightarrow K \ell \nu)$ will yield $|V_{cd}|/|V_{cs}|$ to 1.3%.

3.2.3.3 Inclusive Semileptonic Decays

HQET provides a surprisingly successful description of the lifetimes of charm hadrons and of the absolute semileptonic branching ratios of the D^0 and D_s [24,25]. Isospin invariance of the strong force informs us that $\Gamma_{SL}(D^0) \simeq \Gamma_{SL}(D^+)$ holds up to corrections $\sim \mathcal{O}(\tan^2\theta_C) \simeq 0.05$. Likewise $SU(3)_{Fl}$ symmetry relates $\Gamma_{SL}(D^0)$ and $\Gamma_{SL}(D_s)$, but a priori would allow them to differ by as much as 30%. However HQET tells us that they should agree to within a few percent. A charm factory is the best place to measure absolute exclusive semileptonic charm branching ratios, in particular $\mathcal{B}(D_s \rightarrow X \ell \nu)$ and thus $\Gamma_{SL}(D_s)$, which have never previously been measured.

3.2.4 Combined Results and Implications of the Leptonic and Semileptonic Measurements for CKM

Every weak decay involving leptons depends on both CKM elements and on hadronic matrix elements. We have described in the Sections above a two-part program in which we use CLEO-c data both to calibrate the theoretical tools that will determine the hadronic terms, and to extract the essential CKM elements. Both exercises reach deep into the heart of particle physics, and both help to build the foundation upon which future advances in our field will stand.

We now summarize the results of the “direct” determinations of the CKM elements $|V_{cd}|$ and $|V_{cs}|$ by combining the leptonic and semileptonic measurements. Table 4 puts all the numbers in one place. For this table we have assumed Lattice QCD, validated across a wide range of charm and onium decay measurements in CLEO-c, will provide decay constants with 1% accuracy. We have not taken advantage of improvements in D and D_s lifetimes that presumably will occur in the near future. In the case of semileptonic decays, we use only the pseudoscalar results for which the theory is the most straightforward.

TABLE 4. CLEO-c: Collected Results for $|V_{cd}|$ and $|V_{cs}|$.

Decay Mode	CKM Element	CKM precision
$D_s \rightarrow \mu^+\nu$	$ V_{cs} $	1.9%
$D_s \rightarrow \tau^+\nu$	$ V_{cs} $	1.6%
$D^0 \rightarrow K^-e^+\nu$	$ V_{cs} $	1.6%
$D^+ \rightarrow \mu^+\nu$	$ V_{cd} $	2.3%
$D^0 \rightarrow \pi^-e^+\nu$	$ V_{cd} $	1.7%

Accounting for the correlated lifetime errors between $D_s \rightarrow \mu\nu$ and $D_s \rightarrow \tau\nu$ we conclude that we can determine these CKM elements as follows:

$$\frac{\Delta|V_{cd}|}{|V_{cd}|} = 1.4\% \qquad \frac{\Delta|V_{cs}|}{|V_{cs}|} = 1.1\%. \qquad (7)$$

This brings these elements into the same level of precision as that of the Cabibbo angle. Additional refinements will become available as more semileptonic modes are added in.

We now summarize the impact of the entire suite of CLEO-c measurements on our knowledge of the CKM matrix, taking into account both the direct and the indirect effects described in the introduction to this Section. Just to remind the reader, we reiterate that the CLEO-c program of leptonic and semileptonic measurements has two components: one of calibrating and validating theoretical methods for calculating hadronic matrix elements, which can then be applied to all problems in CKM extraction in heavy quark physics; and one of extracting CKM elements directly from the CLEO-c data. The *direct* results of CLEO-c are the precise determinations of $|V_{cd}|$, $|V_{cs}|$, f_D , f_{D_s} , and the semileptonic form factors. The precision knowledge of the decay constants f_D and f_{D_s} , together with the rigorous calibration of

theoretical techniques for calculating heavy-to-light semileptonic form factors, are required for the direct extraction of CKM elements from CLEO-c but also drive the *indirect* results, namely the precision extraction of CKM elements from experimental measurements of the B_d mixing frequency, the B_s mixing frequency, and the $B \rightarrow \pi \ell \nu$ decay rate measurements which will be done by a combination of efforts spread across Babar, Belle, CDF, D0, BTeV, LHCb, ATLAS, and CMS.

We present the combined projections in Equation (8) below. In the determination of the CKM elements $|V_{td}|$ and $|V_{ts}|$ from B and B_s mixing we have used $|V_{tb}| = 1$. The tabulation also includes improvement in the direct measurement of $|V_{tb}|$ itself which is expected from the Tevatron experiments [26].

Present Knowledge			After CLEO - c		
0.1%	1%	25%	0.1%	1%	5%
7%	16%	5%	1%	1%	3%
36%	39%	29%	5%	5%	15%

(8)

We may use these results to draw broader conclusions about the validity of unitarity in the CKM picture of quark mixing. The second row and the second column of the CKM matrix will be the most precisely determined components of the matrix when the results of CLEO-c, the B-factories, and the collider experiments are combined, and these elements will therefore play a significant role in our evaluation of the CKM paradigm. It is well known, but not always emphasized, that the CKM unitarity can be expressed by any of *six* triangle relations, and although most of these are “squashed” they still contain interesting windows on physics. We refer the reader to Ref. [27] for further discussion of these points.

From the first two rows of the CKM matrix we can test the unitarity of the CKM matrix with the highly squashed ‘ cu ’ triangle, which is equivalent to the orthogonality condition

$$V_{ud}V_{cd}^* + V_{us}V_{cs}^* + V_{ub}V_{cb}^* = 0. \quad (9)$$

With present PDG2000 central values and one sigma errors on CKM elements (shown below in Equation (10)) this condition fails. If the errors are interpreted in a Gaussian sense, the orthogonality condition has only a 0.2% probability of being satisfied by the available data. Strictly speaking, since the errors are mostly theoretical this Gaussian interpretation is not precisely valid, but it nevertheless indicates that there is some level of difficulty with the existing CKM data.

$$V_{CKM}(PDG2000) = \begin{bmatrix} 0.9735 \pm 0.0008 & 0.2196 \pm 0.0023 & 0.0032 \pm 0.0008 \\ 0.224 \pm 0.016 & 1.04 \pm 0.16 & 0.0402 \pm 0.0019 \\ 0.008 \pm 0.003 & 0.044 \pm 0.017 & 0.99 \pm 0.29 \end{bmatrix} \quad (10)$$

We may also test the normality condition on the second row by itself:

$$|V_{cd}|^2 + |V_{cs}|^2 + |V_{cb}|^2 = 1. \quad (11)$$

We know that with PDG2000 values the first row fails this test by 2.4σ . Again, a Gaussian interpretation, with the same caveats as above, would indicate that the data have only a

0.8% chance of being consistent with the normality condition. The second and third rows have errors that are too large at this point to be discriminating. The columns similarly are not highly resolved with current data. We expect that with the projected five to ten fold improvement in the precision of directly measured CKM elements, these unitarity tests will become quite incisive.

3.3 Absolute Hadronic Charm Meson Branching Fractions

3.3.1 Introduction

As outlined in the introduction to this Chapter, there are several thrusts for the CLEO-c charm physics program. One of these thrusts is a series of precision hadronic charm branching fractions that will set the absolute scale for much of the flavor physics done in the next decade. In this Section we outline the current status of the branching fractions that set the absolute branching fraction scale for charm and charmonium, and discuss the physics issues in charm and beauty physics that are or will soon be limited by these measurements.

3.3.2 Current Status

A list of the best measured branching fractions for each charm or charmonium particle species is given in Table 5. We have included the best individual measurements as well as the Particle Data Group (PDG) fit values. These modes are usually used as the scale for all other branching fraction measurements of each species; thus their measurement provides “absolute branching fractions.”

Of the charm hadrons, the D^0 is the best known. The two experiments listed in Table 5 provide by far the most precise measurements. They use the same technique, in which they look at $D^{*+} \rightarrow \pi^+ D^0$ decays and take the ratio of the D^0 decays into $K^- \pi^+$ to the number of decays with only the π^+ from the D^{*+} decay detected. The dominant systematic uncertainty is the background level in the latter sample. In both experiments, the systematic errors exceed the statistical errors. In fact, the PDG may be overstating the precision, as these experiments have systematic errors at the 3% level and the PDG quotes an overall error of 2.3%, while the systematic errors are likely to be correlated. It is doubtful if increased statistics will allow a substantial decrease of the systematic errors using this method.

The D^+ absolute rate is determined by using fully reconstructed D^{*+} decays, comparing $\pi^0 D^+$ with $\pi^+ D^0$ and using isotopic spin symmetry. Thus this rate cannot be determined in principle any better than the absolute D^0 decay rate using this technique. Furthermore, the systematic errors on the relative efficiency error for detecting a slow π^0 versus a slow π^+ needs to be included.

The absolute rate for $D_s^+ \rightarrow \phi \pi^+$ was measured by CLEO II. It is determined by using fully reconstructed B decays into $D^{(*)} D_s^{*+}$ and comparing the rate when the decay products of the D_s^+ are seen, to the rate just using the γ from $D_s^{*+} \rightarrow \gamma D_s^+$. The dominant systematic error is caused by the uncertainty in the background shape when considering the non-reconstructed D_s^+ case. This error is large because the shape is difficult to ascertain.

The $J/\psi \rightarrow \mu^+ \mu^-$ rate is important because it allows the absolute determination of the cross-section for specific b species at hadron colliders. This could in principle be done with

TABLE 5. Current Absolute Branching Fraction Measurements of Charm and Charmonium Mesons.

Decay	Branching Fraction (%)	Fractional Error (%)	Source
$D^0 \rightarrow K^- \pi^+$	$3.82 \pm 0.07 \pm 0.12$	3.6	CLEO [28]
	$3.90 \pm 0.09 \pm 0.12$	3.8	ALEPH [29]
	3.83 ± 0.09	2.3	PDG [17]
$D^+ \rightarrow K^- \pi^+ \pi^+$	$9.3 \pm 0.6 \pm 0.8$	10.8	CLEO [30]
	$9.1 \pm 1.3 \pm 0.4$	14.9	Mark III [31]
	9.1 ± 0.7	7.7	PDG [17]
$D_s^+ \rightarrow \phi \pi^+$	$3.59 \pm 0.77 \pm 0.48$	25.3	CLEO [32]
	3.6 ± 0.9	25.0	PDG [17]
$J/\psi \rightarrow \mu^+ \mu^-$	$5.84 \pm 0.06 \pm 0.10$	2.0	BES [33]
	6.08 ± 0.33	5.4	BES [34]
	5.88 ± 0.10	1.7	PDG [17]
$\psi(2S) \rightarrow \pi^+ \pi^- J/\psi$	31.0 ± 2.8	9.0	PDG [17]

any known decay but final states including J/ψ are particularly easy to trigger and to detect in hadron environments and fortuitously this is the best determined rate. However, careful examination of Table 5 shows that the measurement is systematically limited and the PDG quotes a somewhat better error (1.7%) than the best measurement (2%) allows, where all the other measurements are considerably worse.

The dominant errors on these measurements are systematic and it is not clear how much these measurements can be improved with more data. Generally we expect some improvement but not very large changes.

In CLEO-c, we are blessed with the ability to reconstruct large samples of the process $e^+e^- \rightarrow D\bar{D}$, where both the charm and anti-charm particles are detected. This allows for absolute branching measurements with little systematic error. We project that CLEO-c will determine the absolute scale of D^0 and D^+ decays to better than $\sim 1\%$ and the absolute scale of D_s decays to better than $\sim 2\%$.

Precise knowledge of an absolute branching fraction scale for charm (and charmonium) particles is very important for issues in both charm and beauty physics since b flavored hadrons most often decay into charmed hadrons. Here we review the most crucial issues.

3.3.3 Physics Enabled by Better Charm Hadron Branching Fraction Measurements

3.3.3.1 Value of $|V_{cb}|$

Currently, the best way of determining $|V_{cb}|$ is via the exclusive decay $B \rightarrow D^* \ell^- \bar{\nu}$ [35]. Here one measures the product of the decay width at maximum four-momentum transfer

and a form-factor derived from Heavy Quark Effective Theory (HQET). Data give an error of 3.8% shared almost equally between statistical and systematic sources. To make improvements, an important component to be reduced is the error on the absolute D^0 branching fraction. Soon, with the large data samples being accumulated by BaBar and Belle, this will become the dominant systematic error in the experimental part of the determination. The error in form-factor is expected to be reduced when unquenched lattice gauge calculations are done [36].

It is worth noting that with significant improvements in V_{cb} coupled with knowledge of $f_K\sqrt{B_K}$ from the unquenched, precision lattice calculations that will be available in the next few years, the $\rho - \eta$ constraints from ϵ_K will be greatly enhanced. This will allow ever more powerful comparisons between CP violation in the B and K meson systems in the future.

3.3.3.2 Understanding Two-body B Meson Decays

B meson decays into a charmed (or hidden charm) meson and a light meson have been a testing ground for QCD. These two-body studies depend on the absolute charmed meson branching fractions. For example Heavy Quark Effective Theory (HQET) predicts that the ratio

$$\frac{\Gamma(\bar{B}^0 \rightarrow D^{*+} X^-)}{\Gamma(\bar{B}^0 \rightarrow D^+ X^-)} = 1 \quad , \quad (12)$$

where X^- is any “light” meson [37]. Tests rely on using the absolute D^+ branching fraction and the absolute D^0 branching fractions, because the decay mode most useful for detecting D^{*+} is $\pi^+ D^0$.

Other more specific tests of our understanding rely on comparing B^- decays into a D^0 or D^{*0} with \bar{B}^0 decays into a D^+ or D^{*+} and extracting amplitudes for color allowed and color suppressed transitions [37]. These tests depend on knowledge of absolute branching fractions.

One of the color suppressed decay modes, $J/\psi K^0$, is the first to be used in studies of CP violation. In order to understand the underlying weak physics it is important to understand the strong interaction physics.

Two-body decays such as $\bar{B}^0 \rightarrow D^{*+} D_s^-$ have been used to test factorization and/or predict the decay constant of the D_s meson. Factorization is the hypothesis first stated by Bjorken, that in two-body B decays to light mesons, the W^- can form a color-singlet meson and not participate in the coupling of the spectator quark to the c (or u) quark [38]. This can be tested quantitatively by comparing the two body decays with semileptonic B decays at a four-momentum transfer equal to the mass of the light hadron. These rely on the absolute D_s^+ decay branching fraction that is poorly known [39].

3.3.3.3 The Charm Content in b Decay

Summing the charm yield in B decays has long been used to understand the dynamics of the decays and look for new phenomena [37]. For example, there is a predicted correlation between the semileptonic branching fraction and the rate of $b \rightarrow c\bar{c}s$ decays. Current charm absolute branching fraction measurements limit the quality of these tests [40].

3.3.3.4 Effects on Probes of Beyond SM Physics

Precision measurements of $Z \rightarrow b\bar{b}$, R_b , and $Z \rightarrow c\bar{c}$, R_c , are important tests of the Standard Model. Although LEP has ceased taking data, future linear colliders may re-address this issue. Improving precision of these measurements, indeed even reinterpreting existing measurements, requires better determinations of the absolute branching fractions for charm [41]. Similar arguments can be made for precision Higgs studies at future colliders that will rely on decays $H \rightarrow b\bar{b}$ and $H \rightarrow c\bar{c}$.

3.3.3.5 QCD Models of Heavy Quark Production

The nature of charm and beauty production is the subject of considerable interest [42]. Precision measurement is not possible until the branching fractions are well known. It is not just the absolute rate normalization, but also the Monte Carlo calculations of the detection efficiency ultimately depend on the accuracy of the branching fraction input.

Other lessons can be learned. The baryon yield, in particular can teach us about string fragmentation processes. Until the absolute Λ_c^+ branching fraction is determined more precisely these tests cannot be performed.

3.4 Charm Baryons

We comment briefly on the opportunities presented by CLEO-c data taken at the $\Lambda_c\bar{\Lambda}_c$ threshold.

In the last decade, there has been much progress made on our knowledge of charmed baryon spectroscopy and decays. The number of states for which reasonable mass and width measurements exist is now over twenty. Furthermore, there has been progress made on the understanding of the decay mechanisms of the weakly decaying charmed baryons. Much of this work has been done at CLEO, as the beam energy of around 5 GeV is large enough to produce the full spectrum of charmed baryons, and the superb detector capabilities are well matched to extracting small signals out of the millions of hadronic events.

However, despite the progress, the absolute scale for charm baryon decays is not well determined. To date, the measurements of the charm baryon absolute rate are model dependent. The decay mode chosen to normalize all other decay rates to is $\Lambda_c^+ \rightarrow pK^-\pi^+$. A lower limit on the branching fraction can be obtained assuming that B meson decays to baryons are dominated by the process $\bar{B} \rightarrow \Lambda_c^+\bar{N}X$. Data then yield $\mathcal{B}(\Lambda_c) = (4.14 \pm 0.91)\%$ [17]. An upper limit is obtained using the decays $\Lambda_c^+ \rightarrow \Lambda\ell^+\nu$ and assuming that the Λ final state saturates the rate; then $\mathcal{B}(\Lambda_c) = (7.7 \pm 1.5)\%$ [17]. Combining these results has $9.7\% > \mathcal{B}(\Lambda_c) > 3.0\%$, where the limits are at 90% confidence level. Prospects for improving this situation are dim without data taken near $\Lambda_c\bar{\Lambda}_c$ threshold. With a modest amount of threshold data we can anticipate measuring $\mathcal{B}(\Lambda_c)$ to within 4% of itself.

Semileptonic decays of charm baryons are also of interest in order to test and further probe our theoretical understanding of form factors. No effective symmetry relates $\Gamma_{SL}(D)$, $\Gamma_{SL}(\Lambda_c)$, $\Gamma_{SL}(\Xi_c^0)$ and $\Gamma_{SL}(\Xi_c^+)$. Furthermore contributions of order $1/m_c^2$ and $1/m_c^3$ generate sizable or even large differences between the semileptonic widths of charm mesons and the various charm baryons. Comparing $\mathcal{B}(D \rightarrow X\ell\nu)$ and $\mathcal{B}(\Lambda_c \rightarrow X\ell\nu)$ provides a test of HQET and duality. We also note that measurement of the process $\Lambda_b^0 \rightarrow \Lambda_c^+\ell^-\bar{\nu}$ could eventually

be important in constraining theoretical form-factor uncertainties. This will require precise knowledge of the absolute Λ_c^+ branching ratio as well a determination of the level of Λ_b^0 production [43].

3.5 Charm Beyond the Standard Model

3.5.1 Mixing

Within the Standard Model, the processes which mediate the decays of charmed quarks and antiquarks can change the “charm” quantum number by one unit, $\Delta C = \pm 1$. On the other hand, the mixing of D^0 and \bar{D}^0 necessitates changing a charm quark, c , into an anti-charm quark, \bar{c} , *i.e.*, the “charm” quantum number must change by two units. This can be arranged in the SM only at one loop level and, therefore, is naturally suppressed. However, new physics (beyond Standard Model) contributions can generate $\Delta C = \pm 2$ interactions as well. It is for this reason that neutral meson-antimeson mixing can provide important information about both the Standard Model and new physics beyond the SM. The $D^0 - \bar{D}^0$ system is particularly interesting in this respect as it is the only system that is sensitive to the dynamics of bottom-type quarks.

The motivation most often cited in searches for $D^0 - \bar{D}^0$ mixing is the possibility of observing a signal from new physics which dominates the signal from the Standard Model. The low energy effect of new physics particles can be naturally written in terms of a series of local operators of increasing dimension generating $\Delta C = \pm 2$ transitions. These operators, along with the Standard Model contributions, generate the mass and width splittings for the eigenstates of $D^0 - \bar{D}^0$ mixing matrix defined as

$$|D_{1,2}\rangle = p|D^0\rangle \pm q|\bar{D}^0\rangle \quad , \quad (13)$$

with complex parameters p and q determined from the phenomenological (CPT-invariant) $D^0 - \bar{D}^0$ mass matrix [44]. It is convenient to normalize the mass and width differences and define two dimensionless variables x and y

$$x \equiv \frac{m_2 - m_1}{\Gamma} \quad , \quad y \equiv \frac{\Gamma_2 - \Gamma_1}{2\Gamma} \quad , \quad (14)$$

where $m_i(\Gamma_i)$ is the mass (width) of the corresponding state, D_i . Clearly, y is constructed from the decays of D into physical states, and so it should be dominated by the SM contributions. If CP-violation is neglected, then $p = q$ and $|D_{1,2}\rangle$ become eigenstates of CP .

To set up a relevant formalism, let us recall that in perturbation theory, the element ij of the $D^0 - \bar{D}^0$ mass matrix can be represented as

$$\left[M - i\frac{\Gamma}{2} \right]_{ij} = m_D \delta_{ij} + \frac{1}{2m_D} \langle D_i^0 | \mathcal{H}_W^{\Delta C=2} | D_j^0 \rangle + \frac{1}{2m_D} \sum_I \frac{\langle D_i^0 | \mathcal{H}_W^{\Delta C=1} | I \rangle \langle I | \mathcal{H}_W^{\Delta C=1\dagger} | D_j^0 \rangle}{m_D^2 - E_I^2 + i\epsilon} \quad . \quad (15)$$

Here the first order correction term in Equation (15) comes from the *local* $\Delta C = 2$ (box and dipenguin) operators. These operators would give contributions to the dispersive part of $\left[M - i\frac{\Gamma}{2} \right]_{ij}$, *i.e.*, only affect x . They are expected to be small in the Standard Model [45,46,

47]. It is therefore natural to expect that this part of Equation (15) might receive contributions from the effective operators generated by new physics interactions. The second order correction term of Equation (15) includes bilocal contributions which are induced by the insertion of two Hamiltonians changing the charm quantum number by one unit, *i.e.*, built out of $\Delta C = 1$ operators. This class of terms contributes to both x and y and is believed to give the dominant SM contribution to mixing due to various nonperturbative effects [48]. Some enhancement due to $\Delta C = 1$ operators induced by new physics is also possible, but unlikely given the strong experimental constraints provided by data on D meson decays. Most theoretical estimates suggest that x and y are very small: $x, y \leq 10^{-3}$.

The mass and width differences x and y can be measured in a variety of ways, for instance in semileptonic $D \rightarrow Kl\nu$ or nonleptonic $D \rightarrow KK$ or $D \rightarrow K\pi$ decays. The simplest measurement involves counting the “wrong sign” final states, like l^- or π^- in the decay of a meson initially tagged as D^0 . This procedure unambiguously measures the mixing rate $r = (x^2 + y^2)/2$ for semileptonic final states, while for the $K\pi$ final state it is complicated by the presence of the double-Cabibbo suppressed (DCS) amplitudes $A_{K\pi}$. It is possible to separate DCS amplitudes from the mixing contribution by performing time-dependent studies of $\Gamma(D \rightarrow K\pi)[t]$ [49]. Such time-dependent analysis, however, is not feasible at CLEO-c. Nevertheless, as we will discuss later, the presence of the quantum-coherent state of $D\bar{D}$ at CLEO-c has enormous advantage: DCS amplitudes are absent for some hadronic final states.

There are several intriguing experimental measurements which have used the techniques described above to provide some information about $D^0 - \bar{D}^0$ mixing parameters [50,51,52,53]. One type of analysis [50,51,53] fits the time dependent decay rates of the singly-Cabibbo suppressed (such as $D \rightarrow KK$) and the Cabibbo-favored modes to pure exponentials. The one sigma ranges measured by these experiments are

$$\begin{aligned} y_{\text{CP}}^{\text{FOCUS}} &= (3.42 \pm 1.57) \times 10^{-2} \\ y_{\text{CP}}^{\text{Belle}} &= (1.0_{-3.5}^{+3.8+1.1}) \times 10^{-2} \\ y_{\text{CP}}^{\text{CLEO}} &= (-1.1 \pm 2.5 \pm 1.4) \times 10^{-2} \end{aligned} \quad (16)$$

In addition, CLEO has performed time-dependent studies of $D \rightarrow K\pi$ [52] fitting the coefficient of each of the three terms ($1, \Gamma t$ and $(\Gamma t)^2$). The coefficient of the linear term is proportional to the interference of the mixing and DCS amplitudes and depends on the strong phase difference between direct and DCS amplitudes δ (for a discussion see [54,55,56,57,58]) and possible CP-violating new physics phase ϕ , while the coefficient of the constant term gives the ratio of DCS vs. Cabibbo-favored (CF) decays, R . Such measurements allow a fit to the parameters $R, R_m, x' \sin \phi, y' \cos \phi$, and $x^2 + y^2$, where x' and y' are related to x and y by the strong phase δ : $y' = y \cos \delta - x \sin \delta$ and $x' = x \cos \delta + y \sin \delta$ [49]. CLEO quotes the following one sigma ranges:

$$\begin{aligned} R &= (0.48 \pm 0.13) \times 10^{-2}, \\ y' \cos \phi &= (-2.5_{-1.6}^{+1.4}) \times 10^{-2}, \\ x' &= (0.0 \pm 1.5) \times 10^{-2}. \end{aligned} \quad (17)$$

A combined analysis of x' and y_{CP} provides powerful constraints on the values of $D^0 - \bar{D}^0$ mixing parameters [49].

CLEO-c will have the important experimental advantage of operating at the $D^0\bar{D}^0$ threshold, where the D^0 and \bar{D}^0 mesons are produced in the state that is quantum mechanically coherent. This allows new and simple methods to be used to measure the $D^0 - \bar{D}^0$ mixing parameters [59]. Consider for instance $D^0\bar{D}^0 \rightarrow (K^-\pi^+)(K^-\pi^+)$. The initial $D^0\bar{D}^0$ state is prepared as

$$|i\rangle = \frac{1}{\sqrt{2}} \left\{ |D^0(k_1, t_1)\bar{D}^0(k_2, t_2)\rangle + (-1)^l |D^0(k_2, t_2)\bar{D}^0(k_1, t_1)\rangle \right\} \quad (18)$$

where $l = 1$ at $\psi(3770)$, so the $D^0\bar{D}^0$ system is in the antisymmetric initial state. This implies that in the time-dependent amplitude $A(D^0\bar{D}^0 \rightarrow (K^-\pi^+)^2)$, the DCS amplitude interferes away and does not contribute. Therefore, for $D^0\bar{D}^0$ pairs produced from the decay of the $\psi(3770)$ the time-dependent rate is

$$\Gamma(t) \propto \frac{\Gamma^2}{8} e^{-\Gamma(t_1+t_2)} \left| \frac{p}{q} \right|^2 |B(k_1)|^2 |B(k_2)|^2 (x+y)^2 (t_1-t_2)^2 \quad (19)$$

with $B \equiv B_{K^-\pi^+}$ being the CF decay amplitude. Normalizing to $\Gamma(D^0\bar{D}^0 \rightarrow (K^-\pi^+)(K^+\pi^-))$ which is given by

$$\Gamma(t) \propto \frac{1}{2} e^{-\Gamma(t_1+t_2)} |B_{K^-\pi^+}(k_1)|^2 |B_{K^+\pi^-}(k_2)|^2 \quad (20)$$

implies for the time-integrated ratio

$$\mathcal{R} \left(\frac{(K^-\pi^+)(K^-\pi^+)}{(K^-\pi^+)(K^+\pi^-)} \right) = \frac{x^2 + y^2}{2} \left| \frac{p}{q} \right|^2 \frac{|B_{K^-\pi^+}|^2}{|B_{K^+\pi^-}|^2}. \quad (21)$$

This is similar to the case of semileptonic final states

$$\mathcal{R} \left(\frac{(l^\pm l^\pm)}{(l^\pm l^\mp)} \right) = \frac{x^2 + y^2}{2}, \quad (22)$$

but is free from the experimental drawbacks that are usually associated with semileptonic modes. We note that the DCS amplitude does not cancel for all decay modes. Consider for example $\Gamma(D^0\bar{D}^0 \rightarrow (K^-\pi^+)(K^-\rho^+))$, and for simplicity, set $x = y = 0$. Simple analysis shows [59] that

$$\mathcal{R} \left(\frac{(K^\pm\pi^\mp)(K^\pm\rho^\mp)}{(K^\pm\pi^\mp)(K^\mp\rho^\pm)} \right) = \left| \frac{\bar{A}_{K^-\pi^+}}{B_{K^-\pi^+}} - \frac{\bar{A}_{K^-\rho^+}}{B_{K^-\rho^+}} \right|^2 \neq 0 \quad (23)$$

as $R_{K\pi} \neq R_{K\rho}$. Therefore, the DCSD amplitude persists in this case.

For the case where one final state is hadronic and the other semileptonic,

$$\mathcal{R} \left(\frac{(l^+\nu K^-)(K^-\rho^+)}{(l^+\nu K^-)(K^+\rho^-)} \right) = \left| \frac{\bar{A}_{K^-\rho^+}}{B_{K^-\rho^+}} \right|^2 + \frac{x^2 + y^2}{2}, \quad (24)$$

we can also take advantage of the coherence of the D mesons produced at the ψ'' to extract the strong phase difference between the direct and DCS amplitudes, δ , that appears in the

time dependent mixing measurements. Since the CP properties of the final states produced in the decay of $\psi(3770)$ are anti-correlated, one D state decaying into a final state with definite CP properties immediately identifies or tags the CP properties of the state “on the other side.” If one state decays into, for example, $\pi^0 K_S$ with $CP = -1$, the other state is “CP-tagged” as being in the $CP = +1$ state. This allows one to measure the branching ratio $\mathcal{B}(D_{CP} \rightarrow K^- \pi^+)$ and, as we will see below, $\cos \delta$.

We can write a triangle relation which follows from the definition of D_{CP} ,

$$\sqrt{2}A(D_{CP} \rightarrow K^- \pi^+) = A(D^0 \rightarrow K^- \pi^+) \pm A(\bar{D}^0 \rightarrow K^- \pi^+). \quad (25)$$

This implies

$$1 \pm 2 \cos \delta \sqrt{R} = 2 \frac{\mathcal{B}(D_{\pm} \rightarrow K^- \pi^+)}{\mathcal{B}(D^0 \rightarrow K^- \pi^+)}, \quad (26)$$

where we used the fact that $R \ll \sqrt{R}$ and neglected CP violation in mixing, which could undermine the CP-tagging procedure by splitting the CP-tagged state on one side into a linear combination of CP-even and CP-odd states thus requiring time-dependent studies. Both effects, however, are negligibly small. Now, if both decays of D_+ and D_- are measured, $\cos \delta$ can be obtained from the asymmetry

$$\cos \delta = \frac{\mathcal{B}(D_+ \rightarrow K^- \pi^+) - \mathcal{B}(D_- \rightarrow K^- \pi^+)}{2\sqrt{R}\mathcal{B}(D^0 \rightarrow K^- \pi^+)}. \quad (27)$$

These two expressions can be used to extract δ from independent measurements at CLEO-c.

Thus, in addition to the “standard” methods of searches for $D^0 - \bar{D}^0$ mixing, new tools and methods, unique to running at the $\psi(3770)$ (and higher resonances), become available for studies of these important parameters.

3.5.2 CP Violation

3.5.2.1 Introduction

While CP violation was first observed in the neutral kaon system and has recently been observed in neutral B mesons, the Standard Model predicts very small effects in both charged and neutral charm mesons. Therefore, the Standard Model background to any non-Standard Model physics is much smaller than in the B and K systems, making charm an excellent venue to look for new physics using CP violation as a probe.

3.5.2.2 Direct CP Violation

In addition to indirect CP violation mentioned in the previous Section, both SM and new physics effects can induce different contributions to the *decay amplitudes* of D meson. This phenomenon can be traced back to the appearance of complex-valued couplings (CKM parameters) in the $\Delta C = 1$ Lagrangian that mediates D decays and leads to CP-violating difference between decays rates of CP -conjugated states.

Studies of direct CP violation usually require two different amplitudes having non-trivial weak and strong phase difference to reach a given final state. Final state hadron dynamics must provide non-zero strong phase shifts. Unfortunately, in charm decays, the impact of

the final state hadronic rescattering cannot be described accurately in perturbative QCD. Various models can be called upon, but the predictions are not robust.

Let us consider a decay of a charmed meson. If there are two different amplitudes A_1 and A_2 with associated strong phases δ_1 and δ_2 , then the decay amplitude for $D \rightarrow f$ is given by

$$A_f = A_1 e^{i\delta_1} + A_2 e^{i\delta_2} . \quad (28)$$

For the CP conjugate reaction, $\bar{D} \rightarrow \bar{f}$ the weak phases change but the strong phases stay the same

$$\bar{A}_{\bar{f}} = A_1^* e^{i\delta_1} + A_2^* e^{i\delta_2} . \quad (29)$$

The CP violating asymmetry is given by

$$A_{CP} = \frac{|A_f|^2 - |\bar{A}_{\bar{f}}|^2}{|A_f|^2 + |\bar{A}_{\bar{f}}|^2} = \frac{2Im(A_1^* A_2) \sin(\delta_1 - \delta_2)}{|A_1|^2 + |A_2|^2 + 2Re(A_1^* A_2) \cos(\delta_1 - \delta_2)} . \quad (30)$$

As discussed above, one selects final states that can be reached from at least two different routes. In charmless B -decays the two different weak amplitudes are typically associated with the tree and penguin transitions. As follows from Eq. (30), A_{CP} is directly proportional to the sine of the strong phase difference. While the theoretical status of FSI phases in B decays is not yet settled, in charm decays FSI have been observed. Moreover, final state rescattering effects are appreciably large in the D meson system due to the fact that its mass lies in the middle of the region populated by the light quark resonances [57,54,60]. Therefore, the final state phase does not per se pose a problem for the observation of direct CP violating effects in charmed meson decays. Small expected values for A_{CP} arise in the Standard Model, because the Cabibbo part of the CKM matrix is “almost” unitary, *i.e.*, weak phase effects in charmed decays are tiny, that makes the observation of CP violating effects problematic. However, new physics can vastly enhance charm CP violating asymmetries, thus making charm a very good place for new physics searches [61].

As argued above, A_{CP} is indeed difficult to predict because of the hadronic uncertainties in the amplitudes and strong phases. We note that CP violation is bound to be larger in Cabibbo suppressed decays than in non-suppressed decays. How large can A_{CP} be? It’s been argued that for Cabibbo suppressed decays in cannot be larger than 10^{-3} . This is based on the rephasing-invariant quantity (or Jarlskog invariant)

$$J = Im[V_{ij} V_{kl} V_{ik}^* V_{jl}^*], \quad (31)$$

where any choice of $i \neq l$ and $j \neq k$ is allowed. Using current approximate values for the CKM elements and taking $\sin(\delta_1 - \delta_2)$ equal to one, then for Cabibbo suppressed decays the asymmetry can be as large as 10^{-3} . This is indeed a small asymmetry. Nevertheless, searches for CP violation in charm decays have been going on for quite some time but have reached accuracies of only several percent [53,62].

D_s^+ decays present another situation. Detailed calculations by Buccella *et al.* [63] have some asymmetries in rare decays as large as 3×10^{-3} . In D^+ decays the largest prediction is 8×10^{-3} .

3.5.2.3 Observing CP Violation Through Quantum Correlations at the ψ''

The production process

$$e^+e^- \rightarrow \psi'' \rightarrow D^0\bar{D}^0 \quad (32)$$

produces an eigenstate of CP+, in the first step, since the ψ'' has J^{PC} equal to 1^{--} .

Consider the case where both the D^0 and the \bar{D}^0 decay into CP eigenstates. Then the decays

$$\psi'' \rightarrow f_+^i f_+^j \text{ or } f_-^i f_-^j, \quad (33)$$

are forbidden, where f_+ denotes a CP+ eigenstate and f_- denotes a CP- eigenstate. This is because

$$\text{CP}(f_{\pm}^i f_{\pm}^j) = (-1)^{\ell} = -1 \quad (34)$$

for the $\ell = 1$ ψ'' .

Thus if a final state such as $(K^+K^-)(\pi^+\pi^-)$ is observed, we immediately have evidence of CP violation. Moreover, all CP+ and CP- eigenstates can be summed over for this measurement.

This measurement can also be performed at higher energies where the final state $D^{*0}\bar{D}^{*0}$ is produced. When either D^* decays into a π^0 and a D^0 , the situation is the same as above. When the decay is $D^{*0} \rightarrow \gamma D^0$ the CP parity is changed by a multiplicative factor of -1 and all decays $f_+^i f_-^j$ violate CP symmetry [64].

Even though we are considering D^0 's, we can have direct CP violation here as well as CP violation through mixing. Because we can sum many channels, this study at the ψ'' may provide the most sensitive way to see CP violation in charm decays and could reach the sensitivity to see Standard Model mechanisms.

3.5.2.4 Conclusions

CP violation through mixing is expected to be negligible small in the Standard Model. Direct CP effects in D^0 and D^+ are expected to be at a level no larger than a $\mathcal{O}(10^{-3})$, while they may be up to 10^{-2} in certain suppressed D_s channels. Current measurements of CP violation in D^0 decay are at the several percent sensitivity level [62,65]. The limits are considerably worse in D^+ and D_s decay. There are significant opportunities to search for the effects of new physics via the mechanism of CP violation in the CLEO-c program.

3.5.3 Rare Charm Decays

In this Section we will discuss the motivation for studying rare charm decays. We will give estimates of the reach of both CLEO-c and BaBar for a broad set of these modes in Chapter III.

Rare decays of charmed mesons and baryons provide “background-free” probes of new physics effects. In the framework of the Standard Model (SM) these processes occur only at one loop level. SM predicts vanishingly small branching ratios for these processes because of the absence in the Standard Model of the super-heavy bottom-type quark supplemented by almost perfect GIM cancelation between the contributions of s and d quarks. This is very different from the familiar case of bottom quark decays where the top quark contribution dominates the decay amplitude. It also makes the Standard Model predictions for these

transitions very uncertain, as the perturbative GIM cancelation mechanism is not effective for soft, long-distance contributions. In addition, in many cases annihilation topologies also give sizable contributions. At the end, any anomalous enhancement of a given branching ratio would have to be compared to the (dominant long-distance) Standard Model amplitude. Fortunately, several model-dependent estimates exist indicating that the SM predictions for these processes are still far below current experimental sensitivities. Some examples are given in Table 6. See also [66,67].

New Physics (NP) effects, on the other hand, need not be suppressed. Many models of NP, including supersymmetric extensions of the SM, either involve heavy particles that need not suffer from GIM-type cancelations or include other mechanisms that give appreciable contribution to flavor-changing neutral currents in D -decays. For example, new tree-level flavor-changing interactions amplitudes would contribute [68,69]. Note that many models of New Physics would also affect mixing parameters such as ΔM_D . We refer the reader to the literature for many comprehensive examples [68]. Estimates of the contributions of new physics to rare D decays are also given in Table 6.

We see from Table 6 that experiments that can measure rare D decay branching ratios at the level of 10^{-6} will start to confront models of new physics in an interesting way.

4 Opportunities for Tau Lepton Physics

4.1 Introduction

The tau is the heaviest of the leptons. Largely because of its mass, studies of the properties of the tau lepton can provide input on a number of fundamental questions in particle physics. Some of these include

- Measurements of fundamental quantities (e.g. tau mass, tau neutrino mass) and key tau decay branching fractions;
- Tests of charged weak couplings and lepton universality in leptonic tau decays to $e\bar{\nu}_e\nu_\tau$ and $\mu\bar{\nu}_\mu\nu_\tau$. Deviations from the Standard Model expectations would indicate the presence of new physics;
- Studies of the strong and weak interaction physics of light mesonic systems via semi-hadronic tau decays;
- Direct searches for non-Standard Model physics through forbidden decays, such as those with lepton-flavor nonconservation (like $\tau \rightarrow \mu\gamma$) or those arising from second-class currents (like $\tau \rightarrow \pi\eta\nu_\tau$), or through sensitivity to possible CP nonconservation in allowed decays.

During the 1990's significant progress was made in all of these areas, mainly at e^+e^- colliders running in the Υ energy range (DORIS, CESR) and on the Z^0 peak (SLC, LEP). Due to large datasets and quality detectors, tau physics has now become precision physics. Continuation of this program at energies well above production threshold is expected to continue at the asymmetric B -factories over the next decade.

While the efforts in tau physics at the 'high energy' facilities mentioned above have been quite successful, there exist both unique and complementary capabilities at lower energies.

TABLE 6. Standard Model short distance (SD) and long distance (LD) branching fraction estimates, and New Physics contributions to rare D^0 decay modes.

Decay Mode	SM \mathcal{B}_{SD}	SM \mathcal{B}_{LD}	New Physics
<i>Leptonic</i>			
$D^0 \rightarrow \mu^+ \mu^-$	$(1 - 20) \times 10^{-19}$	$< 3 \times 10^{-15}$	10^{-9} [70]
$D^0 \rightarrow e^+ e^-$			
<i>Photonic</i>			
$D^0 \rightarrow \gamma\gamma$	10^{-16}	$< 3 \times 10^{-9}$	
<i>Radiative</i>			
$D \rightarrow X_u \gamma$	$(4 - 8) \times 10^{-12}$		$10^{-12} - 10^{-6}$ [70,71,72]
$D^0 \rightarrow \rho^0 \gamma$		$(1 - 5) \times 10^{-6}$	
$D^0 \rightarrow \phi^0 \gamma$		$(0.1 - 3.4) \times 10^{-5}$	
<i>FCNC Semileptonic</i>			
$D \rightarrow X_u \ell^+ \ell^-$	4×10^{-9}		
$D^0 \rightarrow \pi^0 \mu\mu$			10^{-9} [70]
$D^0 \rightarrow \bar{K}^0 ee/\mu\mu$		$< 2 \times 10^{-15}$	
$D^0 \rightarrow \rho^0 ee/\mu\mu$			
$D^+ \rightarrow \pi^+ ee/\mu\mu$	$\text{few} \times 10^{-10}$	$< 10^{-8}$	
$D^+ \rightarrow K^+ ee/\mu\mu$		$< 10^{-15}$	
$D^+ \rightarrow \rho^+ \mu\mu$			
<i>FCNC $\nu\bar{\nu}$</i>			
$D^0 \rightarrow X_u + \nu\bar{\nu}$	2.0×10^{-15}		
$D^0 \rightarrow \pi^0 \nu\bar{\nu}$	4.9×10^{-16}	$< 6 \times 10^{-16}$	
$D^0 \rightarrow \bar{K}^0 \nu\bar{\nu}$		$< 10^{-12}$	
$D^+ \rightarrow X_u \nu\bar{\nu}$	4.5×10^{-15}		
$D^+ \rightarrow \pi^+ \nu\bar{\nu}$	3.9×10^{-16}	$< 8 \times 10^{-16}$	
$D^+ \rightarrow K^+ \nu\bar{\nu}$		$< 10^{-14}$	
<i>Lepton-flavor violating</i>			
$D^0 \rightarrow \mu^\pm e^\mp$	0	0	10^{-13} [73]

Some of this physics can be done in conjunction with the charm physics program of CLEO-c, at the ψ' and at higher energies. Other measurements require dedicated running in the τ -pair production threshold region extending from $2 \times m_\tau$ to tens of MeV above. In fact, use of the tau threshold region has always been an integral part of the development of the

‘tau-charm factory’ concept.

In this Section, the physics opportunities of a facility producing tau-pairs at threshold or in the charm region are discussed, with emphasis on those areas where unique capabilities exist. We note that many of the ideas described here on tau physics opportunities at these energies were first articulated in the tau-charm factory studies of the past decade (see Refs. [12,13,14,15,16]). The possible measurements are discussed in the order given by the outline of topics listed above. Studies of the capabilities of the CLEO-c tau physics program are described in the corresponding Section in Chapter III of this document.

4.2 Measurement of Key Tau Lepton Properties

Key properties of the tau lepton include the masses of the tau and the tau neutrino, the tau lepton lifetime, and branching fractions for significant decay modes. The tau lifetime is now known (mainly from LEP experiments) to better than 4 per mil, and is clearly not within the scope of CLEO-c physics capabilities. However, significant and in some cases definitive measurements of the other properties are possible. These are discussed below.

4.2.1 Tau Lepton Mass

The mass of the tau lepton m_τ is a fundamental parameter in the Standard Model. As such, a precise determination would constitute an important archival measurement. It will become important if a future fundamental theory for calculating fermion masses is to be tested. In addition, m_τ plays an important role in the lepton universality tests described below in Section 4.3. Finally, a detailed study of the cross section near threshold could be sensitive to interesting radiative and threshold (such as tauonium formation) effects.

A definitive measurement of m_τ is possible with CLEO-c. By far the most precise determination of m_τ to date is $1776.96^{+0.18+0.25}_{-0.21-0.17}$ MeV [74] from a scan of the threshold region by the BES experiment in 1991. Measurements of m_τ have been made at higher energies by Argus [75] and CLEO [76] based on kinematic considerations. However these experiments report systematic errors at the 1 MeV level. Thus, the best (only?) hope for improving the precision on m_τ is to measure the tau-pair production cross section in a scan of the threshold region, following an approach similar to that used by BES. A dedicated effort with CESR-c/CLEO-c should lead to a determination of m_τ with an overall precision of 0.1 MeV.

4.2.2 Tau Decay Branching Fractions

In Table 7, the dominant Cabibbo-favored tau decay modes are listed, along with the current world average branching fractions [17]. Precise determination of these branching fractions is valuable, with the leptonic and $\pi^- \nu$ decays providing sensitive tests of lepton universality in conjunction with measurements of the tau mass and lifetime as well as the muon and charged pion lifetimes (see Section 4.3). The branching fractions of the semi-hadronic decays provide powerful tests of QCD and strong interaction physics.

In addition, the Conserved Vector Current Theorem (CVC) allows one to relate the partial decay rates and spectral functions of channels produced via the vector part of the weak $V - A$ current to the cross sections for $e^+e^- \rightarrow$ hadrons at low energies (*i.e.*, $s < 4m_\tau^2$).

TABLE 7. World average branching fractions of dominant τ^- decays.

Decay	Branching Fraction (%)
$\nu_\tau \mu^- \bar{\nu}_\mu$	17.37 ± 0.07
$\nu_\tau e^- \bar{\nu}_e$	17.83 ± 0.06
$\nu_\tau \pi^-$	11.09 ± 0.12
$\nu_\tau \pi^- \pi^0$	25.40 ± 0.14
$\nu_\tau \pi^- \pi^+ \pi^-$	9.18 ± 0.11
$\nu_\tau \pi^- \pi^0 \pi^0$	9.13 ± 0.14
$\nu_\tau \pi^- \pi^+ \pi^- \pi^0$	4.20 ± 0.08
$\nu_\tau \pi^- \pi^0 \pi^0 \pi^0$	1.08 ± 0.10

Testing CVC is of general interest, and with the recent acquisition of very high statistics e^+e^- data at Novosibirsk, tests can be carried out to high precision. This is of particular importance in light of applications of tau decay data made possible by CVC. With CVC, tau decays can be used [77] to augment the e^+e^- data in the determination of hadronic vacuum polarization corrections to the anomalous magnetic moment of the muon $a_\mu = (g_\mu - 2)/2$ as well as to the running of the electromagnetic fine structure constant.

Existing data hint at some potential inconsistencies. For example, the measured $\tau^- \rightarrow \pi^- \pi^0 \nu_\tau$ branching fraction from Table 7 is larger than the CVC prediction [78] of $(24.64 \pm 0.29)\%$ based on $e^+e^- \rightarrow \pi^+ \pi^-$ data (including some preliminary data from CMD-2) by $(0.76 \pm 0.32)\%$. This is important because the $\pi\pi$ state accounts for roughly 70% of the total hadronic correction to a_μ . Resolving this apparent inconsistency could have a significant impact [78,79] on the interpretation of the BNL E821 measurement of a_μ , the most recent results from which [80] deviate from the Standard Model prediction by 2.6 standard deviations.

What are the opportunities for CLEO-c in this area? Already the precision on the leptonic and $\pi^- \pi^0 \nu_\tau$ decay modes is in the 4–6 per mil level, and the other modes listed in Table 7 (other than $\pi^- 3\pi^0 \nu_\tau$) have been measured with relative errors in the 1–2 per cent range. Furthermore, the asymmetric B -factory experiments will each obtain samples 10–50 times as large as those used by previous experiments. However, most of the measurements dominating the world averages listed in Table 7 are systematics-limited. Controlling systematics at the sub-1% level will surely be a challenging task for the B -factory experiments. CLEO-c can perform measurements at the 1%-level with very different systematics than those present at higher energies.

For example, the near-monochromatic momentum spectrum of pions from $\tau^- \rightarrow \pi^- \nu_\tau$ near tau threshold allows nearly unambiguous separation of these decays from many other tau decay channels. Consequently, systematic errors present at higher energies associated with the rejection and estimation of feed-across from $\tau^- \rightarrow \pi^- \pi^0 \nu_\tau$ decays (with the photons from the π^0 undetected or overlapping with the difficult-to-model interaction of the π^- in the calorimeter) will be largely absent at CLEO-c. Similarly, other semi-hadronic decays, such as $\tau^- \rightarrow \pi^- \pi^0 \nu_\tau$, can be cleanly identified by making use of the dependence of the

momentum of the hadronic system on its mass on an event by event basis.

Although capabilities exist at CLEO-c to study rarer (*i.e.*, currently statistics limited) decay modes such as those involving kaons, it is unlikely that sufficient luminosity can be attained to permit precision measurements of these channels. For such modes, the asymmetric B -factories will be better positioned to accumulate the required high statistics. However there may be unique modes for which the experimental conditions at CLEO-c are more favorable.

4.2.3 Tau Neutrino Mass

Another fundamental property accessible in tau physics is the mass of the tau neutrino m_{ν_τ} , should this be sufficiently large as to be discernible. Previous tau-charm factory studies have suggested that sensitivity to m_{ν_τ} in the range of 1–5 MeV could be attainable. The experience of the higher energy experiments, as well as studies carried out in the context of this document, suggest that this level of sensitivity will be difficult to attain. However, significant improvement over the current direct limit of 18.2 MeV (95% CL) [81] may be possible with CLEO-c.

4.3 Studies of Weak Couplings and Lepton Universality

4.3.1 Tests of Lepton Universality

The rates for certain exclusive decay channels of the tau lepton are sensitive to small deviations from the universality of couplings in the leptonic charged weak current. Specifically μ - τ universality can be tested in the leptonic decays $\tau^- \rightarrow l^- \bar{\nu}_l \nu_\tau$ via the following relation to muon decay:

$$\left(\frac{g_\tau}{g_\mu}\right)^2 = \frac{\tau_\mu}{\tau_\tau} \left(\frac{m_\mu}{m_\tau}\right)^5 \mathcal{B}(\tau^- \rightarrow e^- \bar{\nu}_e \nu_\tau) (1 + \delta_W) (1 + \delta_\gamma), \quad (35)$$

where g_τ and g_μ are the charged weak coupling constants (equal to $e \sin \theta_W$ in the Standard Model), and δ_W and δ_γ represent well-known weak and EM radiative corrections [82]. This relation tests the transverse W boson couplings [83], while the longitudinal couplings can be tested via comparison of the semi-hadronic decay $\tau^- \rightarrow \pi^- \nu_\tau$ with pion decay:

$$\left(\frac{g_\tau}{g_\mu}\right)^2 = \frac{\tau_\pi}{\tau_\tau} \left(\frac{m_\mu}{m_\tau}\right)^3 \frac{\mathcal{B}(\tau \rightarrow \pi \nu)}{\mathcal{B}(\pi \rightarrow \mu \nu) H(m_\pi, m_\mu, m_\tau, \delta_\pi)}, \quad (36)$$

where

$$H(m_\pi, m_\mu, m_\tau, \delta_\pi) = (1 + \delta_\pi) \left(\frac{1 - m_\pi^2/m_\tau^2}{1 - m_\mu^2/m_\pi^2}\right)^2, \quad (37)$$

and the quantity δ_π is another well-known EM radiative correction [84,85]. Deviations from unity in either Equation (35) or Equation (36) above would be a sign of new physics.

The most likely impact of CLEO-c with regard to the test in Equation (35) is the measurement of m_τ , described in the preceding Section. At present this test is limited at the 0.5% level by the tau lifetime and branching fraction measurements, with m_τ contributing

an uncertainty of about 0.1%. Improving the precision on m_τ will clear the way for a μ - τ universality test at the 10^{-3} level.

The test of longitudinal W boson couplings in Equation (36) is limited at the 1% level by the uncertainty on the $\tau \rightarrow \pi\nu$ branching fraction, and possibly by theoretical uncertainties in the calculation of radiative corrections. Assuming the latter can be improved, a sub 1% measurement of the $\tau \rightarrow \pi\nu$ branching fraction will have an immediate payoff in the precision of this test. Determination of this branching fraction is quite challenging at Υ energies. As mentioned in the previous Section, an improved measurement with different systematic errors would be a valuable contribution from CLEO-c.

4.3.2 Weak Couplings: The Michel Parameters

In addition to the total rate for leptonic decays described above, the shape of the lepton energy spectrum is sensitive to non-Standard Model contributions. In the absence of knowledge of the outgoing lepton polarization, the lepton energy spectrum can be characterized by four Michel parameters ρ , η , ξ and δ :

$$\begin{aligned} \frac{d^2\Gamma}{dx d\cos\theta} \sim & x^2 \left\{ 3(1-x) + \rho \left(\frac{8}{3}x - 2 \right) + 3\eta \left(\frac{m_l}{m_\tau} \right) \left(\frac{1-x}{x} \right) \right. \\ & \left. + P_\tau \xi \cos\theta \left[(1-x) + \delta \left(\frac{8}{3}x - 2 \right) \right] \right\} \end{aligned} \quad (38)$$

in the τ rest frame, where x is the scaled energy of the decay lepton $x = E_l/E_{\max}$, P_τ is the tau polarization and θ is the angle between the decay lepton momentum and the tau spin orientation. The Michel parameters depend on bilinear combinations of ten complex fundamental coupling constants $g_{ij}^{(S,V,T)}$, ($i, j = L, R$) for the possible Lorentz structures for the leptonic weak current: scalar (S), vector (V) or tensor (T), for left- (L) and right-handed (R) couplings. In the Standard Model only the $V - A$ coupling g_{LL}^V is non-zero.

The current status of measurements of the four Michel parameters studied in tau decay is given in Table 8 [17], with values from muon decay and the Standard Model for comparison. The world average values are dominated by the CLEO II measurements, in which the main

TABLE 8. World average values for the Michel parameters in muon and τ^- decay. (The values listed for δ in τ decay are actually for $\xi\delta$.)

Param.	$\mu \rightarrow e\bar{\nu}\nu$	$\tau \rightarrow e\bar{\nu}\nu$	$\tau \rightarrow \mu\bar{\nu}\nu$	SM Value
ρ	0.7518 ± 0.0026	0.749 ± 0.011	0.752 ± 0.021	3/4
η	-0.007 ± 0.013	—	-0.013 ± 0.097	0
ξ	1.003 ± 0.008	0.995 ± 0.044	1.046 ± 0.065	1
δ	0.749 ± 0.004	0.735 ± 0.030	0.774 ± 0.043	3/4

errors are statistical. Thus it is likely that the asymmetric B -factory experiments will be able to make very precise measurements with their large data samples. Measurement of ξ and δ require knowledge of the τ spin orientation, which was achieved by CLEO II [86] via exploitation of spin correlations between the τ^+ and τ^- . At energies near tau threshold, the

spin correlations are different than at energies where the τ 's are highly relativistic. Thus it is possible to measure these parameters with a very different spin structure from what will be encountered by BaBar and Belle.

There is also a unique opportunity for CLEO-c to contribute significantly to the measurement of η in $\tau^- \rightarrow \mu \bar{\nu}_\mu \nu_\tau$. (Note that a non-zero value of η would have a negligible effect on the electronic decay since the term containing η is suppressed by a factor of m_e/m_τ). The η parameter is of great interest since a non-zero value would indicate the likely presence of a scalar current, such as that associated with a charged Higgs boson. Experiments near threshold have a significant advantage in the measurement of η as its impact is confined to the low energy part of the muon momentum spectrum. For experiments at the $\Upsilon(4S)$, the tau boost smears out the effect somewhat, however the bulk of the effect is still at low energies where muon identification is difficult. With CLEO-c, the smearing of the effect is considerably less, and although direct muon identification is not possible for most of the entire spectrum, vetoing of electrons and rejection of semi-hadronic decays based on kinematics and photon vetoes can leave a very pure $\tau^- \rightarrow \mu \bar{\nu}_\mu \nu_\tau$ sample.

4.4 Studies of Hadronic Dynamics in Tau Decays

The production of light hadronic systems via the well-understood weak interaction makes tau decay samples an excellent source of information about the strong interaction dynamics of these systems. Detailed studies of the $2\pi\nu$, $3\pi\nu$ and $4\pi\nu$ decay channels at CLEO-II and the LEP experiments have greatly advanced the understanding of light vector and axial vector meson resonance parameters and decay dynamics. Semi-inclusive spectral functions in semi-hadronic tau decays have been used to extract α_s and test sum rules. There is much more work to be done in this area, for example: (1) tests of CVC, (2) studies of Wess-Zumino anomalous three-meson couplings, (3) tests of chiral perturbation theory, (4) measurement of non-perturbative parameters to aid in the extraction of α_s , (5) tests of sum rules, (6) searches for second class currents in $\tau^- \rightarrow \pi^- \eta \nu_\tau$ and $\tau^- \rightarrow [4\pi]^- \nu_\tau$, and (7) application of hadronic spectral functions to make factorization-based predictions for hadronic B -meson decays. This program will continue at the asymmetric B -factories where very large samples will be obtained for such studies.

In addition, unique opportunities exist with CLEO-c to explore this physics. For example, tests of chiral perturbation theory rely on measuring hadronic systems at low q^2 , where the final state particle momenta are small in the hadronic rest frame. At B -factory energies, the acceptance for such decays is rapidly varying in this region due to small opening angles between particles which cause them to overlap in the detector. At CLEO-c, this will be much less of a problem since the hadronic system in semi-hadronic tau decays is typically produced at much lower energies. As another example, in the use of $\tau^- \rightarrow \pi^- \pi^0 \nu_\tau$ decays to help determine the vacuum polarization corrections to the muon magnetic moment, the result is quite sensitive to the shape of the $M_{\pi\pi}$ spectrum below the $\rho(770)$ peak. With sufficient luminosity, CLEO-c can measure this part of the spectrum with good control over systematic errors.

4.5 Direct Searches for Non-Standard Model Physics

With CLEO-c, many investigations aimed at specific non-Standard Model processes involving tau lepton decays can be pursued. Searches for many forbidden or suppressed channels, such as the neutrinoless decay $\tau \rightarrow \mu\gamma$, have been carried out successfully at CLEO-II with branching fraction sensitivities at the 10^{-6} level. It is unlikely that CLEO-c will be able to compete with the asymmetric B -factory experiments in the next generation of many such searches. However, for decays in which undetectable particles are produced, experiments at higher energies are essentially insensitive. CLEO-c has a clear advantage here, again because of the tau decay kinematics in the threshold region. Elements of a program of exotic tau physics include:

1. Use of the $\pi^-\nu$ decay mode to search for the possible exotic decay with an unknown massive neutrino, $\tau^- \rightarrow \pi^-\nu_X$.
2. Study of the lepton spectrum in $\tau^- \rightarrow e^-\bar{\nu}_e\nu_\tau$ and $\tau^- \rightarrow \mu^-\bar{\nu}_\mu\nu_\tau$ to look for anomalous contributions. An example is the search for a weakly interacting spin 0 or 1 neutral particle G , in the two-body decay $\tau^- \rightarrow e^-G$.
3. Search for of anomalous couplings in the radiative decays $\tau^- \rightarrow e^-\bar{\nu}_e\nu_\tau\gamma$ and $\tau^- \rightarrow \pi^-\nu_\tau\gamma$.
4. Searches for CP violation in tau lepton decays.

These are discussed briefly below.

4.5.1 Search for $\tau^- \rightarrow \pi^-\nu_X$

Searches for additional peaks in the momentum spectrum of muons from pion decay have been suggested [87] as a means of searching for (most likely unconventional) massive neutrinos that mix with ν_μ . Running at tau threshold allows an analogous search for an admixture of massive neutrinos ν_X that mix with ν_τ . Such a search makes explicit use of the monochromatic momentum spectrum of particles produced in two-body decays of τ 's that are at rest, where the momentum of the detected particle (in this case the π^-) provides direct information on the mass of the unobserved particle (the ν_X). Because of the large mass of the tau, a larger range of possible values for m_{ν_X} can be explored. In addition, such decays may be enhanced due to a potentially larger coupling of the ν_X to the third generation leptons.

4.5.2 Search for $\tau^- \rightarrow e^-G$

Similar to the above topic, decays of τ leptons at rest to a weakly interacting possibly massive particle G via a lepton-flavor-changing interaction would give rise to peaks in the electron momentum spectrum in $\tau^- \rightarrow e^- + \textit{nothing}$. One candidate for such a particle is the familon, which is envisioned as a Goldstone boson associated with the family symmetry that gives rise to lepton flavor conservation [88].

4.5.3 Study of the radiative decay $\tau^- \rightarrow e^- \bar{\nu}_e \nu_\tau \gamma$

Radiative tau lepton decays have been studied so far with limited precision [89,90]. Such decays are potentially sensitive to non-Standard Model couplings. The features of tau production and decay near threshold allow exploration of regions of phase space that are difficult to study at higher energies where there are irreducible backgrounds. For example, at threshold radiative effects in tau-pair production are entirely absent (*i.e.*, no initial-state or final-state radiative photons can be produced).

4.5.4 CP Violation in Tau Decay

Searches for possible CP -violating effects in tau-pair production and decay have been undertaken at LEP and at CESR, and will likely be a subject of intensive study at BaBar and Belle. As in the case of the spin-dependent Michel parameters, CLEO II [91] made use of (longitudinal) spin correlations to construct CP -odd observables. At threshold, transverse spin correlations are significant, and consequently observables can be constructed that would be sensitive to different CP -violating effects. In τ decay, CP -violating effects could arise from interference between W -exchange and other (*i.e.*, charged Higgs exchange) processes. Searches in production include measurement of the tau electric dipole moment.

4.6 Summary of Tau Physics Opportunities

In light of the significant advances in tau physics in recent years and the capabilities of the asymmetric B -factory experiments, the CLEO-c tau physics program will not be as broad as the CLEO-II program was. However, CLEO-c is uniquely poised to make several important measurements in tau physics. The highlights of this program include:

- *Precise measurement of the tau lepton mass:*
This will not only provide a valuable second sub-MeV measurement, but should also be a significant improvement over the BES measurement as a ± 0.1 MeV sensitivity is expected. This will also result in a sensitive exploration of the cross section behavior near threshold.
- *Improved constraints on the tau neutrino mass:*
This will depend on the luminosity of CESR-c but in principle sensitivity at the sub-10 MeV level is possible.
- *Precise measurement of key branching fractions:*
CLEO-c measurements of $B(\tau^- \rightarrow \pi^- \nu_\tau)$ and $B(\tau^- \rightarrow \pi^- \pi^0 \nu_\tau)$ will have significantly different systematics from those made at higher energies, due to the unique kinematics in the tau-charm region. In addition, studies of resonant structure and other strong interaction physics can be done with semi-hadronic channels.
- *Measurement of the Michel Parameter η in $\tau^- \rightarrow \mu^- \bar{\nu}_\mu \nu_\tau$:*
Scalar couplings would lead to a non-zero value for η . It is difficult to measure this at higher energies since the boost smears out the part of the Michel spectrum that is sensitive to it, and because muon identification in the sensitive part of the spectrum is difficult.

- *Searches for exotic phenomena in tau decay:*

The nearly monochromatic momentum spectrum in two-body tau decays near threshold make possible sensitive searches that cannot be done elsewhere. The absence of initial- and final-state radiation in tau-pair production near threshold will aid searches for anomalous effects in radiative tau decays. Searches for CP violation, complementary to those done at higher energies, can be carried out near threshold.

5 Nonperturbative QCD

Strongly coupled quantum field theories remain one of the outstanding challenges to contemporary theoretical physics. Since QCD is the only fundamental theory of this sort, its strong coupling sector is particularly interesting to theorists and experimenters alike. The truly novel behavior in QCD is confinement, and confinement is a low-energy, nonperturbative phenomenon, for which *ab initio* calculational techniques, such as LQCD, are still in the early stages of their development. This Section of our project description defines an experimental program that focuses on the nonperturbative structure of QCD, providing the raw material needed to advance our understanding and control over strongly coupled theories in general, and QCD in particular. The advances we make in understanding QCD and calibrating the theoretical methods such as LQCD for calculating nonperturbative phenomena will enhance our ability to extract precision electroweak physics from experiments in the flavor sector.

5.1 Experimental Probes

The CLEO-c experimental program will fill a critical need for detailed experimental data about all sectors of nonperturbative QCD against which calculations can be calibrated and tested. Recent advances in LQCD promise very accurate predictions for a variety of nonperturbative quantities. Current calculations deliver 10-20% accurate results for a wide variety of masses and form factors. The technology is now in hand to provide $\sim 1\%$ accuracy for dozens of calculations in the next few years [8]. CLEO-c will provide measurements with few percent precision to confront these calculations. Strong coupling expansions, although still quite primitive, could become an important complement to LQCD simulations. For example, when string theorists invented a new technique for strong-coupling expansions, one of their first applications was a calculation of QCD glueball masses (ordinary hadrons could not be analyzed) [92]. However they were forced to compare their results to LQCD simulation because there was insufficient experimental data. This situation will change dramatically with the arrival of the data described in this document.

In this Section we will describe how CLEO-c will probe the low energy spectrum of QCD with precision never before possible. QCD predicts very different sorts of bound states in addition to the standard mesons and baryons, in which the gluon is a constituent, as well as providing the binding force. (This is possible because the gluon carries QCD charge – unlike the electrically neutral photon.) Both quark-gluon “hybrid” states, and purely gluonic “glueballs” are expected. Such states are completely new forms of matter; they do not occur in QED or other weakly-coupled gauge theories. Their discovery and study is essential to a

full understanding of QCD, and will be a focus of analyses performed on data taken at the J/ψ resonance.

Data taken on the $\Upsilon(1S)$, $\Upsilon(2S)$ and $\Upsilon(3S)$ resonances before the conversion to low energy running coupled with J/ψ spectroscopy data obtained after the conversion, will provide a rich and efficient testing ground for lattice techniques as will also be described below.

In other Sections of our project description we describe 1-2% tests of CKM unitarity that are independent of, and in some ways orthogonal to, the probes of CKM to search for Beyond Standard Model physics that will be pursued at the B-factories. We also describe measurements of charm meson decay constants and form factors that further probe and validate these theoretical techniques at a level of precision that is essential to their further development. For example, these data can provide tests of heavy quark expansions for charm meson systems, and the stringent calibrations of LQCD using charm meson data are essential to develop the credibility of the lattice techniques for use in the high precision B and D physics of the future.

The CLEO-c program, with the combination of precision measurements in the charm meson sector, precision measurements of charmonium and bottomonium spectroscopy, and the discovery potential to expose new states of matter in the hadron spectra, will provide the most comprehensive and in depth experimental study of nonperturbative QCD in high energy physics.

5.1.1 The $c\bar{c}$ and $b\bar{b}$ States: Well-understood or Not?

While many $c\bar{c}$ and $b\bar{b}$ bound state mesons are well measured and provide the basis of a rich phenomenology, the spectrum is incomplete in many ways. Almost all of the $c\bar{c}$ mesons below $D\bar{D}$ threshold have been found. By contrast, the spectrum of the $b\bar{b}$ bound states below $B\bar{B}$ threshold is surprisingly incomplete with only the 3S_1 states and the lower lying triplet 3P_J states already discovered. Little is known about the strong decays of all but the lowest states.

The next generation of lattice QCD calculations will predict a wide range of properties for *all narrow* $c\bar{c}$ and $b\bar{b}$ properties such as masses, leptonic widths, photonic transition rates, and hyperfine splittings, with unprecedented accuracy $\sim 1\%$. Substantially improved data will be needed to test these predictions, particularly in the Upsilon system where only masses have been determined with significant precision. Table 9 gives a brief overview of the current precision on the leptonic widths, transition rates and hyperfine splittings in the $b\bar{b}$ system from the PDG [17]. We might expect that the lattice calculations will be largely accurate, but some cases will allow a better tuning of simulation parameters and a few cases will allow development of more accurate techniques.

These tests will also be essential in various phenomenological ways. The higher excited states of either $c\bar{c}$ or $b\bar{b}$ allow more detailed study of the confinement potential and allow tests of the importance of relativistic treatments. In addition, these are the most stringent tests of the simulation techniques for c and b quarks, and will therefore establish the ability of theory to make precision predictions for the D and B systems. The leptonic widths test techniques used to calculate f_B and f_D , and photonic transitions test techniques used to calculate semi-leptonic form factors. Finally, a variety of models will be much more strictly constrained from both these data. We envision a healthy interchange of ideas and methodologies between

empirical models and the lattice calculations.

TABLE 9. The current status of measurements of selected bottomonium resonance parameters from the Particle Data Book [17].

Resonance	Parameter	Current Precision
$\Upsilon(1S)$	Γ	3.4%
	Γ_{ee}	4%
$\Upsilon(2S)$	Γ	16%
	Γ_{ee}	6%
	$\mathcal{B}(\Upsilon(2S) \rightarrow \gamma\chi_b(1P))$	10 – 20%
$\Upsilon(3S)$	Γ	13%
	Γ_{ee}	12%
	$\mathcal{B}(\Upsilon(3S) \rightarrow \gamma\chi_b(2P))$	5 – 11%
$\chi_b(1P)$	$\mathcal{B}(\chi_b(1P) \rightarrow \gamma\Upsilon(1S))$	$\sim 20\%$ or greater
$\chi_b(2P)$	$\mathcal{B}(\chi_b(2P) \rightarrow \gamma\Upsilon(nS))$	15 – 50%
$\chi_b(2P)$	Hyperfine Mass Splittings	4%

It is important to compare both the precision $c\bar{c}$ and $b\bar{b}$ data with calculations since, in principle, theory should provide accurate predictions in both systems despite the large difference in constituent mass. High statistics runs on the $\Upsilon(1S)$, $\Upsilon(2S)$ and $\Upsilon(3S)$ resonances before the conversion of CESR to low energy operation will provide 2-3% measurements of the leptonic widths for the $\Upsilon(nS)$ states, and a whole host of precision decay branching ratios [93]. After the conversion to low energy running data will be taken to allow precision measurement of the same properties of the $c\bar{c}$ states.

5.1.2 Exotica: Searches for New Forms of Matter

It is highly likely that new hadrons with constituent gluons exist since gluons, like u and d quarks, are effectively massless particles that carry QCD charge. Properties of glueballs [94] and hybrid mesons have been predicted in both lattice [95,96,97] and model calculations [11]. The lack of strong evidence for these states is a fundamental issue in QCD spectroscopy. If these states exist, there should be a whole family of states that will tell us important new information about long-range properties of QCD. If the states don't exist, theory *must* account for this unexpected development.

The discovery of exotica is experimentally very challenging. Because gluons have much larger QCD charges than quarks, the lowest mass glueballs and hybrid mesons are expected to be significantly more massive than conventional hadrons. Various lattice calculations have established the idea that hybrid mesons have masses at least 1 GeV/c² above their conventional partners, and that the spectrum of glueball states populates the 1.5 - 2.5 GeV/c² mass range. Consequently these exotic states occur in energy ranges that have not yet been studied carefully. We are far from a complete understanding of the mass spectra, de-

cay branching fractions and microscopic structure of the (presumably non-exotic) hadronic resonances already discovered in the mass range where the lowest lying exotic states are expected to be produced. In addition, the discovery of exotica is complicated by the observation that exotic states with conventional quantum numbers will mix with nearby $q\bar{q}$ states and may have large decay widths. Sorting out the constituent composition of the hadronic states, both conventional and exotic, in the 1-2 GeV/c² mass range will be a necessary part of the experimental program. We refer the reader to PDG reviews [17] for more detailed information.

The current experimental situation is quite murky. Although various claims have been made, there have been no definitive discoveries of exotic states to date. Recent data for light hybrids have come from hadronic beams [98,99,100] rather than e^+e^- machines. Exotic states (1^{-+}) have been tentatively identified at ~ 1.4 GeV/c² and 1.6 GeV/c² through partial wave analysis (PWA). Models and lattice calculations disagree with these data in both mass and decay properties [101].

A search for the lowest mass glueball (0^{++}) in the spectrum of scalar mesons has been one of the primary efforts of the Crystal Barrel experiment at LEAR [102]. They do PWA for $p\bar{p} \rightarrow \pi X$ where X decays to various two-meson pairs. They find three 0^{++} states where models predict only two. Calculations suggest [103,104] that each of these states is a mixture of glueball and conventional meson but the situation is still unresolved. The unconfirmed $f_J(2220)$ is considered a tensor glueball candidate (the mass is quite close to the quenched lattice value [94]) but the current experimental evidence is mutually contradictory and inconclusive [102,105,106,107].

There are two strategies for searching for exotic states. The first strategy is to search for exotic states by finding states with conventional quantum numbers that cannot be accommodated in the established quark multiplet structure that is expected from models. By matching a large portion of the existing meson spectrum, models hope to empirically establish a definitive spectrum of conventional states to compare with the experimental spectrum. Currently lattice calculations do not provide information about the excited conventional hadronic states. However, to establish states as exotic (*i.e.*, not possible in quark models) will require more than just a determination of their masses and quantum numbers. As pointed out above, the claim that a state is supernumerary will require a better understanding of the conventional meson states already found. To accomplish this, a broad range of experimental tools will be required at both CLEO-c and other labs. The advantages of CLEO-c include copious production of glue-rich states in J/ψ radiative decay, the ability to anti-search for glue-rich states in the ‘glue-poor’ environment of two-photon collisions, the ability to look for production of both glue-rich and hybrid states in radiative $\Upsilon(1S)$ decays, and the ability to look for continuum production of states via direct e^+e^- annihilation. Many final states can be examined using the excellent photon calorimeter and tracking capabilities of the CLEO detector.

The second strategy for searching for exotic states is to look for mesons with exotic quantum numbers, quantum numbers that cannot be constructed with $q\bar{q}$ pairs. Simply determining the quantum numbers of such a hadron is sufficient to claim discovery of a non- $q\bar{q}$ state. However a combination of detailed calculations and experimental measurements will be required to prove it is a hybrid, rather than a more conventional, but still interesting, multi-quark state. For example, hybrid states should have a multiplet structure such as is

found for conventional mesons.

It is widely believed that the most efficient way to produce hybrid mesons made with light quarks is likely to be in photoproduction with a hydrogen target through the use of a spin 1 probe at a high enough energy to guarantee t-channel exchange. Dedicated experiments are being proposed for this purpose at TJNAF [108] and at the GSI accelerator in Germany. The TJNAF program hopes to produce physics starting in 2007. We regard these experiments as complementary to the expected studies at CLEO-c which will search for hybrid mesons made from both heavy and light quarks via a variety of production mechanisms.

Partial wave analysis (PWA) is required for many of the analyses that will be done to search for exotic states. Many successful techniques have been developed for analysis of previous experiments, e.g. essentially all data on hadrons in the PDG has resulted from PWA [17]. In some cases, when the initial state quantum numbers are unconstrained, the PWA are very sophisticated. However, CLEO-c data can use well-established techniques for situations when the initial state is fixed such as those developed for Crystal Barrel (LEAR) [102]. For e^+e^- collisions the intermediate state has the quantum numbers of the photon. With $\gamma\gamma$ collisions, the spin and parity are more flexible but still constrained. *Simultaneous* analysis of data from a variety of final states is very important to establish the reliability of any discoveries.

5.1.2.1 Searches for Exotics: Glueballs

The lowest mass glueball state is predicted in many calculations to have $J^{PC} = 0^{++}$ with mass $\sim 1.5 - 1.7 \text{ GeV}/c^2$. As articulated above, this folds glueball searches into the wider problem of understanding the scalar mesons. Figure 1 shows the excited state glueball spectrum from quenched lattice calculations [94]. These results are especially interesting because the excited state structure was determined for the first time.

Unfortunately, in spite of many years of experimental and theoretical progress in the field of light hadron spectroscopy, we lack a complete understanding of the mass spectrum, the branching fractions and the exact constituencies of the hadronic resonances in this energy region. Models provide an accurate picture of the masses and widths for a few dozen mesons of masses less than $2.1 \text{ GeV}/c^2$ and prominent decay widths. On the other hand, there are a few poorly understood hadrons listed in PDG [17]. These resonances do not fit in the quark model as applied to the SU(3) flavor sector. Some of these hadrons, such as $\eta(1295)$ and $\eta(1440)$, are thought to be radial excitations of conventional mesons; others, such as $f_J(1710)$ and $f_J(2220)$, are glueball candidates. Yet others are resonances, for example $f_0(1370)$ and $f_0(1500)$, whose existence is no longer questioned by the elementary particle physics community; but whose origins remain a mystery [109].

High statistics J/ψ data will help to clarify this situation. Tens (and in some cases hundreds) of thousands of events will be reconstructed in a wide variety of decay modes in CLEO-c for these poorly understood states, allowing determination of their quantum numbers via PWA, as well as measurements of their widths and decay branching fractions. In addition the study of these states in the high statistics 10.58 GeV two-photon data available to CLEO will be crucial in determining their gluonic content through the determination of their two photon couplings.

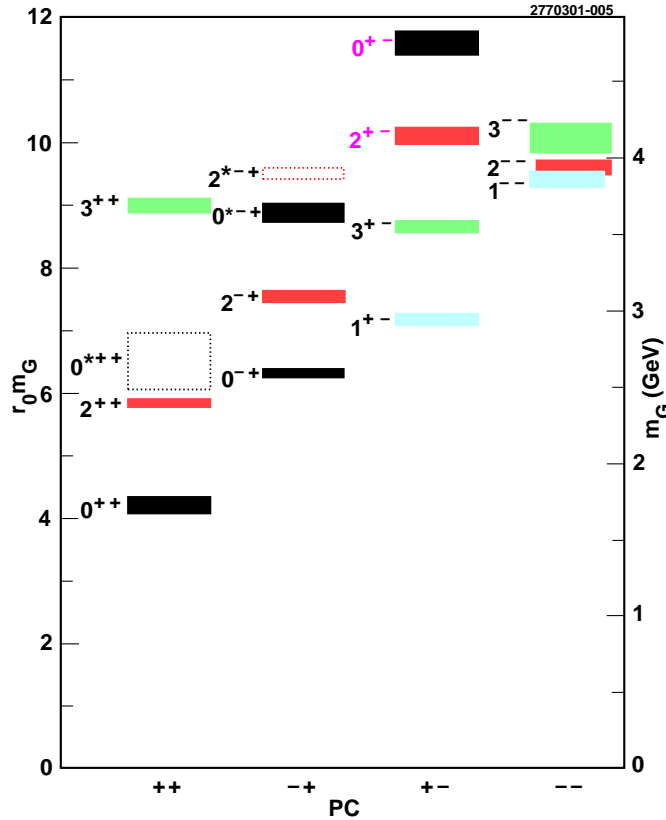


FIGURE 1. The calculated glueball spectrum from [94].

5.1.2.2 Searches for Exotics: Hybrids

The $c\bar{c}$ and $b\bar{b}$ excited states above $D\bar{D}$ and $B\bar{B}$ threshold are largely unstudied. Although the observed states have masses that are consistent with phenomenological quark models, the decay patterns are very odd [110]. The masses, decay widths and branching fractions of these states may be useful for developing the lattice QCD methods for unstable states, since phenomenological potential models seem to be able to predict their masses.

However, the greatest interest in the region above $D\bar{D}$ and $B\bar{B}$ threshold is the opportunity to identify extra states, not part of the spectrum of radial excitations for $c\bar{c}$ or $b\bar{b}$ which may be candidates for 1^{--} hybrid ($c\bar{c}g$ or $b\bar{b}g$) states.

Another possibility is to look for exotic states before the conversion to low energy operation. CLEO will consider a scan in center-of-mass energy in the region above $\Upsilon(4S)$ to search for states not accommodated in the spectrum of $b\bar{b}$ excitations. Also before the conversion, a 1 fb^{-1} $\Upsilon(1S)$ data set will be collected. This will allow us to search for $c\bar{c}g$ hybrid states with a variety of quantum numbers, J^{PC} , which should be produced in $\Upsilon(1S)$ decay. The advantage here is that there will be no restriction on the quantum numbers of the states produced. There is as yet little theoretical guidance on the decay modes to search for although there is prejudice toward decays involving η mesons [111]. The cleanest experimental decay modes are e^+e^- or $\mu^+\mu^-$. The signal will be an extra bump in the dilepton spectrum beyond those predicted by the quark-potential model and lattice simulations for conventional 1^{--} states. If a study of the invariant mass spectrum of dilepton pairs in $\Upsilon(1S)$

decay reveals hybrid candidates, we will search for these states through direct production in e^+e^- annihilation after the low energy conversion.

5.1.3 Physics Running at the $\psi'(3686)$

The physics of the $\psi'(3686)$, the 2^3S_1 $c\bar{c}$ vector meson, is even less “established” than that of the J/ψ . To date the world’s sample of ψ' decays numbers only about 6 million, with a third of these from Crystal Ball data and two thirds from BES. BEPC/BES also hope to produce ~ 16 million additional ψ' in the near future. At CLEO-c a three month run at $\sqrt{s} = 3686$ MeV would produce 50-100 million ψ' . Some of the physics questions of great interest [112] involving the ψ' are

- radiative transition rates,
- searches for missing or unconfirmed states (η'_c and h_c),
- flavor-tagging decays to conventional mesons and exotica, and
- hadronic branching fractions.

The physics reach of CLEO-c for these topics is under active investigation.

5.1.3.1 Radiative transitions

There are ten charmonium radiative transitions that can be accessed starting from the ψ' . Five of these proceed directly from the ψ' itself: the two M1 transitions $\psi' \rightarrow \eta'_c\gamma$ and $\psi' \rightarrow \eta_c\gamma$, and the three E1 transitions to the 3P_J states $\psi' \rightarrow \chi_{cJ}\gamma$. The remaining five are secondary radiative transitions, namely the three E1 transitions $\chi_{cJ} \rightarrow (J/\psi)\gamma$ and the two M1 transitions $\eta'_c \rightarrow (J/\psi)\gamma$ and $J/\psi \rightarrow \eta_c\gamma$. For reference see Figure 2.

The six E1 transitions are classic tests of the quark model, and agree reasonably well with theoretical expectations. However the current experimental accuracy [17] is typically only 10-20%. An improvement of these rates to an accuracy of $\sim 1\%$ would be possible at CLEO-c. This is interesting not only as a test of theoretical predictions, but also because outstanding problems with experimental product branching fractions can be traced to a possible inaccuracy in previous measurements of these E1 transition rates.

The M1 transition rates are much smaller, with the decays $J/\psi \rightarrow \eta_c\gamma$ and $\psi' \rightarrow \eta_c\gamma$ both having partial widths [17] of ~ 1 keV/c² (accidental agreement). The “allowed” transition $J/\psi \rightarrow \eta_c\gamma$ is a very straightforward quark model prediction, so the factor of roughly 2 discrepancy between theory and experiment here is therefore quite surprising. However this experimental partial width is only 3σ from zero, so an improved measurement of $J/\psi \rightarrow \eta_c\gamma$ would be very important. As detailed below, M1 transitions could also be a useful approach for identifying the missing η'_c .

Finally, the “hindered” M1 transitions $\psi' \rightarrow \eta_c\gamma$ and $\eta'_c \rightarrow (J/\psi)\gamma$ are of interest because they have zero partial width in the lowest-order quark model, and hence are sensitive tests of higher-order effects such as different short-distance behavior in the 1^{--} and 0^{-+} $c\bar{c}$ wavefunctions due to the spin-spin (hyperfine) term.

5.1.3.2 Searches for missing $c\bar{c}$ states

The η'_c will be produced in “allowed” M1 radiative transitions from the ψ' . This rate can be determined directly from the $J/\psi \rightarrow \eta_c\gamma$ rate. Assuming identical 1^{--} and 0^{-+} spatial

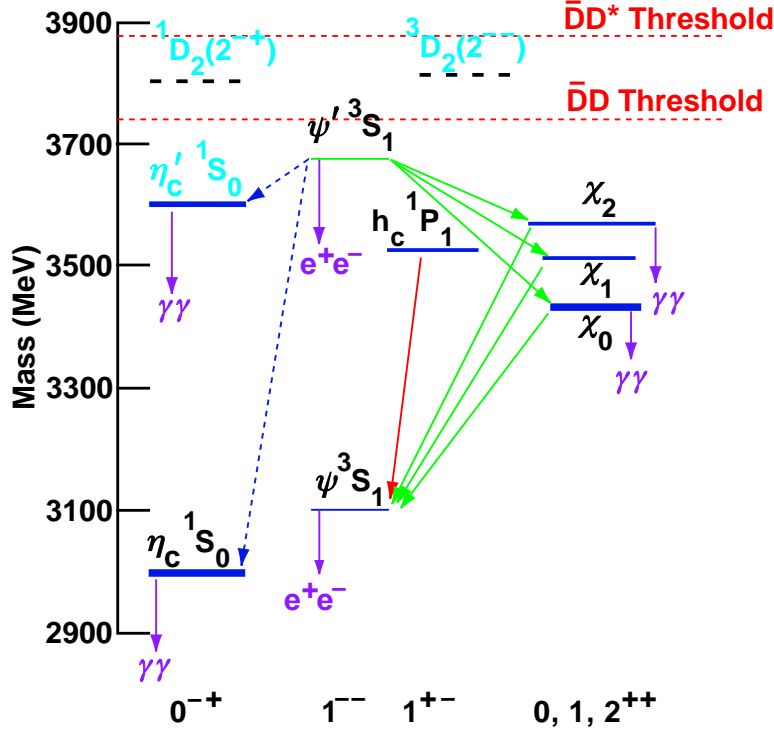


FIGURE 2. Level diagram for the charmonium system, showing some of the main transitions. Other important photon transitions are $\eta_c' \rightarrow \gamma(J/\psi)$ and $J/\psi \rightarrow \gamma\eta_c$.

wavefunctions, these simply scale as k_γ^3 of the photon, so

$$\Gamma(\psi' \rightarrow \eta_c' \gamma) = \left(\frac{(M_{\psi'}^2 - M_{\eta_c'}^2)/2M_{\psi'}}{(M_{J/\psi}^2 - M_{\eta_c}^2)/2M_{J/\psi}} \right)^3 \Gamma(J/\psi \rightarrow \eta_c \gamma). \quad (39)$$

For an η_c' mass of 3630 MeV/c² we expect a partial width $\Gamma(\psi' \rightarrow \eta_c' \gamma)$ of about 0.1 keV or $\mathcal{B}(\psi' \rightarrow \eta_c' \gamma) \sim 5 \times 10^{-4}$. Clearly this rate falls rapidly as the η_c' mass approaches the ψ' mass, and the soft M1 photon might be difficult to identify as a clear peak if the η_c' is broader than the η_c .

Although the spin-singlet 1P_1 state $h_c(3526)$ was reported by E760 at Fermilab in $p\bar{p}$ annihilation [113], the statistics were not large enough to be certain about this result. More recent, higher-statistics studies at E835 have not yet confirmed this discovery. A search for this missing state would be an important CLEO-c contribution. Because the h_c has $J^{PC} = 1^{+-}$ it cannot be made by a one-photon radiative transition from the ψ' . One must instead search for it in suppressed strong decays, such as the isospin-violating mode $\psi' \rightarrow \pi^0 h_c$. In that the h_c is expected to be rather narrow, it may appear in the inclusive π^0 spectrum from ψ' decays, much as the χ_c states can be seen as peaks in the photon energy spectrum in $\psi' \rightarrow \gamma\gamma(J/\psi)$.

The h_c is especially interesting theoretically because its mass has implications for the Lorentz nature of confinement. With *scalar* confinement the only spin-spin force is the one-gluon-exchange (OGE) contact interaction, and as a result the 1P_1 state will lie at the *c.o.g.* of the 3P_J multiplet. When the h_c was reported at only ~ 1 MeV/c² from this mass,

this was considered a dramatic and satisfying success of the model of scalar confinement. Alternatively, with *vector* confinement there is a $1/r$ spin-spin force, and the 1P_1 state is displaced upwards from the 3P_J *c.o.g.* by about $20 \text{ MeV}/c^2$. A better determination of the mass of the h_c is thus of importance for studies of the nature of confinement, which is one of the most interesting questions in nonperturbative QCD.

5.1.3.3 Exotica from hadronic decays of ψ' and χ_c

The traditional approach to glueball searches using charmonium is to study hadronic final states in radiative J/ψ decays. Here, after photon emission, the $c\bar{c}$ annihilation can go through C -even gg states, and hence may have a strong coupling to the low-lying glueballs. To date the unusual states found using this technique are [17] the $\eta(1440)$ (too light to be a glueball?), the $f_0(1710)$ (glueball status still unclear), and the $f_J(2220)$ (controversial and detailed elsewhere in this project description).

A second approach to searching for interesting final states is the use of “flavor-tagging” J/ψ hadronic decays. Here one studies for example $J/\psi \rightarrow VF$, where V is one of the light vectors (ω, ϕ, ρ^0) and F is the exclusive final state of interest. The dominant modes are ones in which F has the same flavor as the final vector V , because isolated final hairpin diagrams are suppressed. Thus $J/\psi \rightarrow \phi F$ shows us what states F can be made by an $s\bar{s}$ source. As expected, one sees strong $J/\psi \rightarrow \omega f_2(1270)$ and $J/\psi \rightarrow \phi f'_2(1525)$ transitions, but the mismatched flavor decays $J/\psi \rightarrow \omega f'_2(1525)$ and $J/\psi \rightarrow \phi f_2(1270)$ are absent [17]. With high statistics this flavor-tagging approach should give very interesting results for both J/ψ and ψ' decays.

An extension of this technique would allow us to probe higher masses and other channels. First, the flavor tagging modes $\psi' \rightarrow VF$ can be investigated; with the ψ' one has sufficient phase space to extend the study well above $2 \text{ GeV}/c^2$ in m_F . Another interesting possibility is to use the rather large radiative modes $\psi' \rightarrow \gamma\chi_c$ to study flavor-tagged χ_c decays. Measurement of the initial E1 photon will select among the three χ_c states, and the flavor-tagged modes $\chi_c \rightarrow VF$ with $V = \omega, \phi$ will give us access to the C -odd spectrum including the 1^{--} and exotic 2^{+-} channels. We also note that $\chi_{c1} \rightarrow \pi F$ decays access, via S -wave, states of $J^{PC} = 1^{-+}$, which are the quantum numbers of the only reported exotic particles [98,114,115].

5.1.3.4 Hadronic branching fractions

There is a long-standing problem in ψ' strong decays, known as the “ $\rho - \pi$ puzzle”. Although $\rho\pi$ is the largest hadronic final state in J/ψ decay, with $\mathcal{B}(J/\psi \rightarrow \rho\pi) \sim 1.3\%$, this final state is unobserved for ψ' , with a limit $\mathcal{B}(\psi' \rightarrow \rho\pi) < 8.3 \times 10^{-5}$ at 90% CL. Similar differences exist in other VP modes.

Despite much speculation, it is actually not clear what this difference means, and the difficult calculation of the transition $ggg \rightarrow VP$ has not been carried out. The simplest approach is to assume that these partial widths are all proportional to the wavefunction at contact squared (as in orthopositronium), in which case the VP widths are approximately given by $\Gamma_{VP}(\psi') \sim 0.5 \times \Gamma_{VP}(J/\psi)$. This would imply a ratio of absolute branching fractions of about 0.2, far from the *limit* of $1/150$ noted above. Clearly there is a major difference between the physics of J/ψ and ψ' annihilation decays.

Measurements of the various strong branching fractions of the ψ' into light hadrons will be of interest as clues regarding the annihilation mechanism, since most of the hadronic modes of the ψ' are poorly measured or are only known as upper limits. We can hope that improved data might lead to a better theoretical understanding of these annihilation decays; they are certainly not understood at present.

5.1.4 Summary

We plan a systematic study of the meson sector in CLEO-c. Although it will be unique, the information obtained will have interesting complementarity with that expected to be obtained at other labs. CLEO-c will utilize a variety of tools, namely J/ψ radiative decays, two-photon collisions (using almost real as well as highly virtual space-like photons), deep inelastic Coulomb scattering and continuum production via e^+e^- annihilation to obtain significant new information on the spectrum of hadrons, both normal and exotic, and their decay channels. We expect qualitative improvement not only from the large statistics we plan to accumulate, but also, even more importantly, from combining the results obtained using all these tools together with the results of our projected $\Upsilon(1S)$, $\Upsilon(2S)$ and $\Upsilon(3S)$ runs. The significance of this is better sensitivity, reduced systematics and a better chance to obtain a coherent picture of the hadron sector.

5.2 Measurement of R

The measurement of the total cross section of e^+e^- annihilation into hadrons is usually referred to as the R measurement. R is the hadronic cross section, corrected for initial state radiation, and normalized to the lowest order QED cross section of the reaction $e^+e^- \rightarrow \mu^+\mu^-$:

$$R = \frac{\sigma^{(0)}(e^+e^- \rightarrow \text{hadrons})}{\sigma^{(0)}(e^+e^- \rightarrow \mu^+\mu^-)}.$$

R measurements can be utilized to measure α_s and to test perturbative QCD. Through dispersion relations they provide the only input to the calculations of the hadronic corrections to the anomalous magnetic moment of the muon $(g-2)_\mu$ [116,117] as well as the value of the running fine structure constant $\alpha(s)$, particularly its magnitude at the Z^0 mass $\alpha(M_Z)$ [116,117,118] which is very important for the global electroweak fits. The current accuracy of such calculations is limited by the systematic uncertainty of the low energy R measurements, the dominant error coming from the ρ meson and the c.m. energy between 1 and 5 GeV. The recent precise measurements of the exclusive hadronic channels by CMD-2 [119] and SND [120] below 1.4 GeV and the R measurement by BES between 2 and 5 GeV with the average systematic uncertainty of 7% [121] had a significant impact on the calculations of $(g-2)_\mu$ [122,123] and $\alpha(M_Z)$ [124]. Further high precision measurements aimed at the determination of R with an accuracy of better than 3–5% in the above energy range would be crucial for, among other studies, high precision tests of the Standard Model and searches for Higgs bosons.

Footnotes and References

1. N. Cabibbo, Phys. Rev. Lett. **10**, 531 (1963).
2. M. Kobayashi and T. Maskawa, Prog. Theor. Phys. **49**, 652 (1973).
3. BaBar Collaboration, B. Aubert *et al.*, Phys. Rev. Lett. **87**, 091801 (2001) [arXiv:hep-ex/0107013].
4. Belle Collaboration, K. Abe *et al.*, Phys. Rev. Lett. **87**, 091802 (2001) [arXiv:hep-ex/0107061].
5. See the topical review article “Quantum Chromodynamics” in Particle Data Group, D. Groom *et al.*, Eur. Phys. J. C **15**, 1 (2000).
6. G. P. Lepage and P. B. Mackenzie, Phys. Rev. D **48**, 2250 (1993).
7. See for example: M. Alford *et al.*, Phys. Lett. B **361**, 87 (1995); M. Luscher *et al.*, Nucl. Phys. B **478**, 365 (1996).
8. Cornell Workshop on High-Precision Lattice QCD, January 2001.
9. I. Bigi, M. Shifman and N. Uraltsev, Ann. Rev. Nucl. Part. Sci. **47**, 591 (1997) [hep-ph/9703290]; M. Neubert, Phys. Rept. **245**, 259 (1994) [hep-ph/9306320].
10. G. T. Bodwin, E. Braaten and G. P. Lepage, Phys. Rev. D **51**, 1125 (1995) [Erratum-ibid. D **55**, 1125 (1995)] [hep-ph/9407339].
11. See, for example: P. R. Page, E. S. Swanson and A. P. Szczepaniak, Phys. Rev. D **59**, 034016 (1999) [hep-ph/9808346]; N. Isgur and J. Paton, Phys. Rev. D **31**, 2910 (1985); N. Isgur and J. Paton, Phys. Lett. B **124**, 247 (1983).
12. SLAC-0343 *Proc. of Tau-Charm Factory Workshop, Stanford, CA, May 23-27, 1989*.
13. J. . Kirkby and J. M. Quesada, *Workshop on Tau charm Factory Detector and Machine, Sevilla, Spain, June 1-6, 1993*.
14. J. . Kirkby and R. Kirkby, *Third Workshop on the Tau charm Factory, Marbella, Spain, June 1-6, 1993*. Gif-sur-Yvette, France: Ed. Frontieres (1994).
15. F. Gilman, Tau/Charm Workshop Summary, Argonne, IL, June 21-23, 1995.
16. M. L. Perl and P. C. Kim, SLAC-PUB-8094 *Summary of the Tau-charm Physics Workshop, Stanford, CA, 6-9 Mar 1999*.
17. D. Groom *et al.*, Eur. Phys. J. C **15**, 1 (2000).
18. C. Bernard, (Lattice 2000) Nucl. Phys. Proc. Suppl. **94**, 159 (2001) [hep-lat/0011064].
19. BES Collaboration, J. Z. Bai *et al.*, Phys. Lett. B **429**, 188 (1998).
20. CLEO Collaboration, M. Chadha *et al.*, Phys. Rev. D **58**, 032002 (1998) [arXiv:hep-ex/9712014].
21. L3 Collaboration, M. Acciarri *et al.*, Phys. Lett. B **396**, 327 (1997).
22. M. Suzuki in Ref. [17].
23. I.I. Bigi, M. Shifman, N. Uraltsev, Ann. Rev. Nucl. Part. Sci. **47**, 591 (1997), with references to earlier work.
24. I.I. Bigi, in *Proceedings of BCP3*, edited by H.-Y. Cheng, W.-S. Hou, (World Scientific, Singapore, 2000), and references therein.
25. G. Bellini, I. Bigi, P. Dornan, Phys. Rep. **289**, 1 (1997).

26. J. Swain and L. Taylor, hep-ph/9712420, hep-ph/9712421.
27. A. Sanda and I. Bigi, hep-ph/9909479.
28. CLEO Collaboration, M. Artuso *et al.*, Phys. Rev. Lett. **80**, 3193 (1998).
29. ALEPH Collaboration, R. Barate *et al.*, Phys. Lett. B **408**, 469 (1997).
30. CLEO Collaboration, R. Balest *et al.*, Phys. Rev. Lett. **72**, 2328 (1994).
31. MARK III Collaboration, J. Adler *et al.*, Phys. Lett. B **196**, 107 (1988).
32. CLEO Collaboration, M. Artuso *et al.*, Phys. Lett. B **378**, 364 (1996).
33. BES Collaboration, J. Z. Bai *et al.*, Phys. Rev. D **58**, 092006 (1998).
34. BES Collaboration, J. Z. Bai *et al.*, Phys. Lett. B **355**, 374 (1995).
35. M. Artuso, “The quest for the Cabibbo Kobayashi Maskawa Matrix,” hep-ph/0012172, (2001). Presented at BEAUTY 2000, to appear in proceedings.
36. A. S. Kronfeld, “B and D Mesons in Lattice QCD”, Mini-review from XXXth Int. Conf. on High Energy Physics, Osaka, Japan (2000), hep-ph/0010074 and references contained therein.
37. T. E. Browder, K. Honscheid, and S. Playfer, in *B Decays, 2nd Edition*, edited by S. Stone, (World Scientific, Singapore 1994), and references contained therein.
38. J. Bjorken, Nucl. Phys. B (Pro. Suppl.) **11**, 325 (1989).
39. D. Bortoletto and S. Stone, Phys. Rev. Lett. **65**, 2951 (1990).
40. H. Yamamoto, “Charm Counting and B Semileptonic Branching Fraction,” presented at 8th Heavy Flavour Conference, Southampton, UK, July 1999, hep-ph/9912308 and reference contained therein.
41. I. Dunietz *et al.*, hep-ph/9606327 (1996).
42. P. Nason *et al.*, in Report of the 1999 CERN Workshop on SM physics (and more) at the LHC, hep-ph/0003142; M. L. Mangano, Presented at the International School of Physics ‘E. Fermi,’ Course CXXXVII, Heavy Flavour Physics, a Probe of Nature’s Grand Design, hep-ph/971137.
43. The level of b -baryon production can be ascertained by reconstructing exclusive B^- and B^0 final states, such as $J/\psi K^-$ and $J/\psi K_S^0$, where the branching fractions are known; then determining the B_s fraction by measuring the rate of like-sign dileptons due to mixing. Total b quark production can be determined studying detached vertices, leptons from detached vertices and the lifetimes of the b species The difference between the total and the sum of B^0 , B^- and B_s is due to b -baryons. It may be possible to disentangle the smaller expected level of Ξ_b production from Λ_b production using lifetime measurements should they differ.
44. See, for example, J. F. Donoghue, E. Golowich and B. R. Holstein, *Dynamics of the standard model* (Cambridge Univ. Press 1992).
45. A. A. Petrov, Phys. Rev. D **56**, 1685 (1997).
46. A. Datta and M. Khambakhar, Z. Phys. C, **27** (1985) 515.
47. J. F. Donoghue, E. Golowich, B. Holstein and J. Trampetic, Phys. Rev. D **33**, 179 (1986).
48. H. Georgi, Phys. Lett. B, **297** (1992) 353; T. Ohl *et al.*, Nucl. Phys. B **403**, 605 (1993); E. Golowich and A. A. Petrov, unpublished; E. Golowich, talk at the Workshop on

- CP Violation, Adelaide, Australia, July 3 - 8, 1998; I. I. Bigi and N. G. Uraltsev, hep-ph/0005089; E. Golowich and A. A. Petrov, Phys. Lett. B **427**, 172 (1998) [hep-ph/9802291].
49. S. Bergmann, Y. Grossman, Z. Ligeti, Y. Nir and A. A. Petrov, Phys. Lett. B **486**, 418 (2000) [hep-ph/0005181].
 50. FOCUS Collaboration, J. M. Link *et al.*, hep-ex/0004034.
 51. BELLE Collaboration, H. Tajima *et al.*, hep-ex/0102016.
 52. CLEO Collaboration, R. Godang *et al.*, hep-ex/0001060.
 53. A. B. Smith for the CLEO Collaboration in *Proceedings of the Fourth International Conference on B Physics & CP Violation*, hep-ex/0104008.
 54. A. F. Falk, Y. Nir and A. A. Petrov, J. High Energy Phys. **9912**, 019 (1999) [hep-ph/9911369].
 55. L.-L. Chau and H.-Y. Cheng, Phys. Lett. B **333**, 514 (1994).
 56. L. Wolfenstein, Phys. Lett. B **164**, 170 (1985).
 57. F. Buccella, M. Lusignoli and A. Pugliese, Phys. Lett. B **379**, 249 (1996).
 58. G. Blaylock, A. Seiden and Y. Nir, Phys. Lett. B **355**, 555 (1995).
 59. I. I. Bigi and A. I. Sanda, Phys. Lett. B **171**, 320 (1986); M. Gronau, Y. Grossman and J. L. Rosner, hep-ph/0103110.
 60. E. Golowich and A. A. Petrov, Phys. Lett. B **427**, 172 (1998) [hep-ph/9802291]; E. Golowich, Phys. Rev. D **24**, 676 (1981).
 61. E. Golowich and A. A. Petrov, in preparation; M. Golden and B. Grinstein, Phys. Lett. B **222**, 501 (1989).
 62. FOCUS Collaboration, J. M. Link *et al.*, Phys. Lett. B **491**, 232 (2000) [Erratum-ibid. B **495**, 232 (2000)] [hep-ex/0005037]; CLEO Collaboration, G. Bonvicini *et al.*, Phys. Rev. D **63**, 071101 (2001) [hep-ex/0012054].
 63. F. Buccella *et al.*, hep-ph/9212253 (1992).
 64. I.I. Bigi and A. I. Sanda, *CP Violation*, Cambridge (University Press, Cambridge, UK 2000) p. 180.
 65. CLEO Collaboration, D. Cronin-Hennessy *et al.*, hep-ex/0102006.
 66. S. Fajfer, S. Prelovsek, P. Singer and D. Wyler, Phys. Lett. B **487**, 81 (2000) [hep-ph/0006054].
 67. G. Burdman, E. Golowich, J.L. Hewett and S. Pakvasa, Phys. Rev. D **52**, 6383 (1995) [hep-ph/9502329].
 68. S. Pakvasa, hep-ph/9705397.
 69. M. Leurer, Phys. Rev. Lett. **71**, 1324 (1993) [hep-ph/9304211]; S. Davidson, D. Bailey and B.A. Campbell, Z. Phys. C **61**, 613 (1994) [hep-ph/9309310].
 70. K.S. Babu, X.G. He, X. Li and S. Pakvasa, Phys. Lett. B **205**, 540 (1988).
 71. S. Prelovsek and D. Wyler, hep-ph/0012116.
 72. I.I. Bigi, F. Gabbiani and A. Masiero, Z. Phys. C **48**, 633 (1990).
 73. G.G. Volkov, V.A. Monich and B.V. Struminsky, Yad. Fiz. **34**, 435 (1981).
 74. BES Collaboration, J.Z. Bai *et al.*, Phys. Rev. D **53**, 20 (1996).

75. ARGUS Collaboration, H. Albrecht *et al.*, Phys. Lett. B **292**, 221 (1992).
76. CLEO Collaboration, A. Anastassov *et al.*, Phys. Rev. D **55**, 2559 (1997). CLEO Collaboration, R. Balest *et al.*, Phys. Rev. D **47**, 3671 (1993).
77. R. Alemany, M. Davier and A. Höcker, Eur. Phys. J. C **2**, 123 (1998).
78. S. Eidelman, presentation at the Workshop on e^+e^- Physics at Intermediate Energies, SLAC, April 30 – May 2, 2001 and private communication. See also S. Eidelman, presentation at the Sixth International Workshop on Tau Lepton Physics, Victoria, September 2000, <http://tau2000.phys.uvic.ca/>.
79. CLEO Collaboration, S. Anderson *et al.*, Phys. Rev. D **61**, 112002 (2000).
80. BNL E821 Collaboration, H. N. Brown *et al.*, hep-ex/0102017.
81. Aleph Collaboration, R. Barate *et al.*, Eur. Phys. J. C **2**, 395 (1998).
82. W. J. Marciano and A. Sirlin, Phys. Rev. Lett. **61**, 1815 (1988).
83. W. J. Marciano, in *Proceedings of the Second Workshop on Tau Lepton Physics*, edited by K. K. Gan, (World Scientific, Singapore, 1993), p. 502.
84. R. Decker and M. Finkemeier, Phys. Lett. B **344**, 199 (1994).
85. W. J. Marciano and A. Sirlin, Phys. Rev. Lett. **71**, 3629 (1993).
86. CLEO Collaboration, J. P. Alexander *et al.*, Phys. Rev. D **56**, 5320 (1997).
87. R. E. Shrock, Phys. Rev. D **24**, 1232 (1981).
88. F. Wilczek, Phys. Rev. Lett. **49**, 1549 (1982); D. B. Reiss, Phys. Lett. B **115**, 217 (1982); G. B. Gelmini, S. Nussinov and T. Yanagida, Nucl. Phys. B **219**, 31 (1983).
89. CLEO Collaboration, M. S. Alam *et al.*, Phys. Rev. Lett. **76**, 2637 (1996).
90. CLEO Collaboration, T. Bergfeld *et al.*, Phys. Rev. Lett. **84**, 830 (2000).
91. CLEO Collaboration, P. Avery *et al.*, CLNS 01/1703, hep-ex/0104009, April 2001, submitted to Phys. Rev. D.
92. R. de Mello Koch *et al.*, Phys. Rev. D **58**, 105009 (1998); C. Csaki *et al.*, JHEP**9901**, 017 (1999).
93. D. Besson and T. Skwarnicki, Ann. Rev. Nucl. Part. Sci **43**, 333 (1993).
94. C. J. Morningstar and M. J. Peardon, Phys. Rev. D **60**, 034509 (1999) [hep-lat/9901004].
95. UKQCD Collaboration, T. Manke, I. T. Drummond, R. R. Horgan and H. P. Shanahan, Nucl. Phys. Proc. Suppl. **63**, 332 (1998) [hep-lat/9709001].
96. MILC Collaboration, C. Bernard *et al.*, Phys. Rev. D **56**, 7039 (1997) [hep-lat/9707008].
97. C. J. Morningstar, K. J. Juge and J. Kuti, Nucl. Phys. Proc. Suppl. **73**, 590 (1999) [hep-lat/9809098];
98. E852 Collaboration, D. R. Thompson *et al.*, Phys. Rev. Lett. **79**, 1630 (1997) [hep-ex/9705011].
99. VES Collaboration, G. M. Beladidze *et al.*, Phys. Lett. B **313**, 276 (1993).
100. Crystal Barrel Collaboration, A. Abele *et al.*, Phys. Lett. B **446**, 349 (1999).
101. T. Barnes, F.E. Close, P.R. Page, and E.S. Swanson, Phys. Rev. D **55**, 4157 (1997), C. Morningstar, hep-ph/0009314, D. Toussaint, hep-lat/9909088.
102. C. Amsler *et al.*, Phys. Lett. B **342**, 433 (1995), **353**, 571 (1995), and **355**, 425 (1995); A. Abele *et al.*, Phys. Lett. B **385**, 425 (1996).

103. C. Amsler and F. E. Close, Phys. Rev. D **53**, 295 (1996) [hep-ph/9507326].
104. J. Sexton, A. Vaccarino, and D. Weingarten, Phys. Rev. Lett. **75**, 4563 (1995).
105. BES Collaboration, J. Z. Bai *et al.*, Phys. Rev. Lett. **76**, 3502 (1996).
106. BES Collaboration, J. Z. Bai *et al.*, Phys. Rev. Lett. **81**, 1179 (1998).
107. MARK III Collaboration, R. M. Baltrusaitis *et al.*, Phys. Rev. Lett. **56**, 107 (1986).
108. Hall D Collaboration, <http://dustbunny.physics.indiana.edu/HallD/>.
109. C. Amsler, Rev. Mod. Phys. **70**, 1293 (1998) [hep-ex/9708025].
110. F. E. Close and P. R. Page, Phys. Lett. B **366**, 323 (1996) [hep-ph/9507407].
111. F. Close, I. Dunieta, P.R. Page, S. Veseli, and H. Yammamoto, Phys. Rev. D **57**, 5653 (1998).
112. E. Eichten, *et al.*, Phys. Rev. D **17**, 3090 (1978); E. Eichten, *et al.*, Phys. Rev. D **21**, 203 (1980); these are two good general reviews of the charmonium model and experimental questions.
113. E760 Collaboration, T.A. Armstrong, *et al.*, Phys. Rev. Lett. **69**, 2337 (1992).
114. S. U. Chung, *et al.*, Phys. Rev. D **60**, 092001 (1999).
115. MPS Collaboration, G.S. Adams, *et al.*, Phys. Rev. Lett. **81**, 5760 (1998).
116. S. Eidelman and F. Jegerlehner, Z. Phys. C **67**, 585 (1995).
117. M. Davier and A.Höcker, Phys. Lett. B **435**, 427 (1998).
118. H. Burkhardt and B. Pietrzyk, Phys. Lett. B **356**, 398 (1995).
119. R.R. Akhmetshin *et al.*, hep-ex/9904027;
R.R. Akhmetshin *et al.*, Nucl. Phys. A **675**, 424c (2000).
120. M.N. Achasov *et al.*, hep-ex/0010077;
M.N. Achasov *et al.*, Phys. Rev. D **63**, 072002 (2001).
121. J.Z. Bai *et al.*, Phys. Rev. Lett. **84**, 594 (2000);
J.Z. Bai *et al.*, hep-ex/0102003.
122. F. Jegerlehner, hep-ph/0104304.
123. S. Eidelman, Workshop on e^+e^- Annihilation at Intermediate Energies, SLAC, April 30 - May 2, 2001.
124. H. Burkhardt and B. Pietrzyk, LAPP-EXP-2001-03.